

**PERFORMANCE AND COST ANALYSES OF HYBRID
DIESEL-PV POWERED SMALL BRACKISH
WATER RO SYSTEMS IN SAUDI ARABIA**

BY

Abdulmajeed Khalid Al-Rubayan

**A Thesis Presented to the
DEANSHIP OF GRADUATE STUDIES**

KING FAHD UNIVERSITY OF PETROLEUM & MINERALS

DHAHRAN, SAUDI ARABIA

**In Partial Fulfillment of the
Requirements for the Degree of**

MASTER OF SCIENCE

In

MECHANICAL ENGINEERING


December 2018

KING FAHD UNIVERSITY OF PETROLEUM & MINERALS

DHAHRAN- 31261, SAUDI ARABIA

DEANSHIP OF GRADUATE STUDIES

This thesis, written by **Abdulmajeed Khalid Al-Rubayan** under the direction of his thesis advisor and approved by his thesis committee, has been presented and accepted by the Dean of Graduate Studies, in partial fulfillment of the requirements for the degree of **MASTER OF SCIENCE IN MECHANICAL ENGINEERING.**



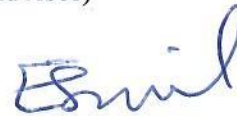
Dr. Zuhair Gasem
Department Chairman



Dr. Salam A. Zummo
Dean of Graduate Studies



Dr. Fahad Al-Sulaiman
(Advisor)



Dr. Esmail M. A. Mokheimer
(Member)



Dr. Mohammed A. Antar
(Member)

31/12/18

Date

© Abdulmajeed Khalid Al-Rubayan

2018

Dedication

To my parents, who taught me how to stand up.

To my hope (my wife), who helped me to stay standing.

ACKNOWLEDGMENTS

I would like to express my thanks to Allah for giving me power and health to complete this work. In addition, I am grateful to King Abdulaziz City for Science and Technology (KACST) for giving me the opportunity and fund to complete my master degree. I am also grateful to King Fahd University of Petroleum & Minerals and Mechanical Engineering Department for giving me this opportunity to pursue my Ms. Program. Furthermore, I would like to express my gratitude to my advisor Dr. Fahad Al-Sulaiman for his support, guidance and patient. Sincere thanks go to both the members of my committee, Dr. Esmail Mokheimer and Dr. Mohamed Antar for their assistance and their useful comments throughout the research.

I take this opportunity to express my deep gratitude to Dr. Mohamed Al-Ghoul, Dr. Ridha Ben Mansour, Dr. Faizur Rahman from KFUPM, Dr. Abdulah Aba-Alkhail, Eng. Moteb Al-Qahtani from Ministry of Environment, Water and Agriculture (MEWA), Eng. Ibrahim Al-Rugaybah from the National Water Company (NWC) and my brother Eng. Abdurhman Al-Rubeaan for their supports throughout my research.

TABLE OF CONTENTS

ACKNOWLEDGMENTS	iii
LIST OF FIGURES.....	vii
LIST OF TABLES.....	viii
LIST OF ABBREVIATIONS.....	ix
ABSTRACT	xii
ملخص الرسالة	xiv
Chapter 1: Introduction	1
1.1. Introduction.....	1
1.2. Water Resources and Categories	1
1.3. Water Demand	5
1.4. Desalination Definition and Methods.....	6
1.4.1. Reverse Osmosis Desalination System	7
1.5. Power Sources.....	13
1.5.1. Diesel Generator	14
1.5.2. Photovoltaic Cells	14
1.5.3. Electrical Batteries	15
1.5.4. Energy Recovery Devices (ERD)	15
1.6. Motivations	16
1.7. Objectives	17
1.8. Methodology	17
Chapter 2: Literature Review	19
2.1. Introduction.....	19
2.2. Reliability and Performance Studies.....	19
2.3. Effect of Parameters Studies	21
2.4. Techno-economic Studies	24
Chapter 3: Mathematical Model and Validation	31
3.1. Introduction.....	31
3.2. Mathematical model	31
3.2.1. Energy/Power Equations:	32
3.2.2. Power/Pressure Equations	35

3.2.3.	Pressure/RO Equations	38
3.2.4.	Economic Equations	42
3.3.	Validation of the model.....	46
Chapter 4:	Performance and Cost Analyses for Ummluj Well	48
4.1.	Introduction	48
4.2.	Data Collection.....	52
4.3.	RO System Design for First Case	53
4.3.1.	Membranes and Pressure Vessels Design	54
4.3.2.	ROSA Results	58
4.4.	Energy Optimization for First Case	61
4.4.1.	ERD Calculation	61
4.4.2.	Load Information	61
4.4.3.	Energy Source Information and Emission	63
4.5.	Economic Study for First Case	64
4.5.1.	RO Economics	65
4.5.2.	Energy Sources Economics	67
4.5.3.	Results for First Case	69
4.6.	Results for other cases.....	71
4.6.1.	Benefit of adding second storage tank	71
4.6.2.	Batch Mode Vs. Continuous Mode	72
4.6.3.	Cases Comparison	75
4.6.4.	Effect of fuel price	78
Chapter 5:	Analyses of Five Different Locations in KSA	81
5.1.	Introduction	81
5.2.	Locations Data	84
5.3.	Energy Consumption for each system	84
5.4.	Results	87
5.4.1.	Effect of Environmental Resources on the Results	87
5.4.2.	LCOW for Different PV Penetration	88
5.4.3.	LCOE for Each System	90
5.4.4.	Effect of Fuel Price	91
5.4.5.	Effect of Second Storage Tank Salinity	93

Chapter 6:	Conclusion and Recommendations	96
6.1.	Conclusion	96
6.2.	Recommendations.....	98
References	99
Vitae	103

LIST OF FIGURES

Figure 1. Water Resources Allocation	2
Figure 2. Water Stress Index in 2015 [2]	3
Figure 3. The water consumption in KSA in 2015 [3]	5
Figure 4. Classification of Common Desalination Processes	7
Figure 5. Direct and Reverse Osmosis Process	8
Figure 6. Basic Components of RO System.....	9
Figure 7. Configuration of Spiral Wound Membrane Element [1].....	11
Figure 8. Pressure Exchanger Components [6].....	16
Figure 9. RO Modes and Cases in This Study	50
Figure 10. Study Flow Chart	51
Figure 11. RO System with Two Tanks and PX.....	56
Figure 12. RO System with One Tank.....	57
Figure 13. RO System Summary.....	58
Figure 14. ROSA Results	59
Figure 15. HOMER Load Information	62
Figure 16. System Schematic.....	63
Figure 17. RO Cash Flow Chart	66
Figure 18. RO Annualized Cash Flow Chart	66
Figure 19. Fuel Consumption and Output Power Relation	68
Figure 20. PV Cost Curve	68
Figure 21. LCOW Curve for Batch Mode, Two Tanks with PX	70
Figure 22. Batch Mode Vs. Continuous Mode (a:One Stage without PX, b:One Stage with PX ,c:Two Stages)	74
Figure 23. LCOW Vs. PV Penetration for Batch Mode Cases.....	76
Figure 24. LCOW Vs. PV Penetration for Continuous Mode Cases.....	77
Figure 25. Water Recovery and SEC for Different Options	77
Figure 26. LCOW for Different Fuel Price at 100% Generator Penetration.....	79
Figure 27. Different Fuel Prices Comparison for Batch Mode, Two Stages System	80
Figure 28. Different Fuel Prices Comparison for Continuous Mode, Two Stages System	80
Figure 29. Locations of Five Wells.....	83
Figure 30. LCOW Vs. PV Penetration for Batch Mode Systems.....	89
Figure 31. LCOW Vs. PV Penetration for Continuous Mode Systems.....	90
Figure 32. LCOE for Different Locations at 100% PV Penetration	91
Figure 33. Breakeven Points for Different Locations for Batch Mode	92
Figure 34. Effect of Second Storage Tank Salinity on the LCOW for Different Locations at 100% PV Batch Mode	94
Figure 35. Effect of Second Storage Tank Salinity on the SEC for Different Locations at 100% PV Batch Mode	95

LIST OF TABLES

Table 1. Water Resources Distribution [4].....	4
Table 2. Water Categories [4]	4
Table 3. Summary of RO parameters [1]	11
Table 4 Summary of some previous works	29
Table 5. Input Validation Data	47
Table 6. Validation Power Results	47
Table 7. Validation Economic Results.....	47
Table 8. Well and Production Information	52
Table 9. Environmental Data [36]	53
Table 10. Membrane Characteristics.....	54
Table 11. Pumps Power Consumptions	60
Table 12. Fuel Properties	64
Table 13. Energy and Emission Information	64
Table 14. RO System Cost Data	65
Table 15. Generator Cost Data.....	68
Table 16. Battery Cost Data	69
Table 17. Detailed Cost Results for Batch Mode, Two Tanks with PX	70
Table 18. Benefit of using Second Storage Tank	72
Table 19. Environmental Data for Five Locations [36]	85
Table 20. Feed Pump Consumption and SEC for Different Locations	86
Table 21. Effect of Environmental Resources on the LCOW and PV System Size for 100% PV Penetration	88
Table 22. Effect of Second Storage Tank Salinity on the RO Design	94

LIST OF ABBREVIATIONS

Symbol	Definition	Unit
A	Area	m^2
An	Equivalent Annual Cost	\$
B	Salt Diffusion Coefficient	$\frac{m^3}{m^2 \cdot h}$
C	Salinity	ppm
c	Concentrate	-
CC	Capital Cost	\$
DC	Direct Capital Cost	\$
E_B	Battery Energy	J
ERD	Energy Recovery Device	-
F	Derating Factor	-
f	Feed	-
FF	Fouling Factor	-
G	Incident Solar Irradiance	$\frac{W}{m^2}$
g	Gravity Acceleration	$\frac{m}{s^2}$
Gen	Generator	-
h	Height	m
HP	High Pressure Pump	-
i	Interest Rate	-
j	Escalation Rate	-

K	Permeability Coefficient	$\frac{m^3}{m^2 \cdot h \cdot bar}$
$LCOE$	Levelized Cost of Energy	$\frac{\$}{Wh}$
$LCOW$	Levelized Cost of Water	$\frac{\$}{m^3}$
\dot{m}	Mass Flow Rate	$\frac{kg}{s}$
N_E	Number of Elements	-
NPV	Net Present Value	\$
Op	Operation Cost	\$
P	Power	W
p	Pressure	bar
pf_{avg}	Concentration Polarization Factor	-
pr	Permeate	-
PV	Photo-Voltaic	-
Q	Flow Rate	$\frac{m^3}{h}$
Q_{cap}	Water Production Capability	$\frac{m^3}{day}$
RO	Reverse Osmosis	-
R_t	Net Cash Flow at That Time	\$
SEC	Specific Energy Consumption	$\frac{Wh}{m^3}$
STC	Standard Test Condition	-
T	Temperature	$^{\circ}C$
t	Time	s

TCF	Temperature Correction Factor	-
Tr	Transportation	-
V_{fuel}	Fuel Volume used per day	$\frac{L}{day}$
α_p	Cell Temperature Coefficient	$\frac{\%}{^{\circ}C}$
η	Efficiency	-
π	Osmotic Pressure	bar
ρ	Density	$\frac{kg}{m^3}$
τ	Availability	-
ΔH^0_{comb}	Net Calorific Value	$\frac{J}{kg}$

ABSTRACT

Full Name : [Abdulmajeed Khalid Al-Rubayan]
Thesis Title : [Performance and Cost Analyses of Hybrid Diesel-PV Powered Small Brackish Water RO System in Saudi Arabia]
Major Field : [Mechanical Engineering]
Date of Degree : [December 2018]

Many wells in Saudi Arabia have high salinity water, which is not directly usable. The aim of this study is to find the best hybrid diesel-PV powered reverse osmosis (RO) systems to desalinate brackish water that has 6000 *ppm* salinity for five different remote areas in the kingdom: Ummluj, Buraydah, Haddar, Qaryat Al-Ulya and Suhmah. Each RO system produces $202 \frac{m^3}{day}$ for two purposes: drinking and household purpose. Two RO modes are studied: batch mode that operates 5 hours a day and continuous mode that operates 24 hours a day. In each mode, the advantages of adding second storage tank for household applications, the advantages of adding second stage and the effect of using pressure exchanger (PX) are studied. In addition, the effect of fuel price is analyzed. The systems are modeled using ROSA and HOMER softwares. It is found that adding second storage tank for household applications with 1000 *ppm* reduces the levelized cost of water (LCOW) by 11%. Furthermore, using PX leads to 26% reduction in the specific energy consumption (SEC) while adding a second stage reduces the SEC by 22%. However, adding PX is economically feasible in continuous mode only. In addition, the optimum RO design is the two stages. If the PV penetration is less than 40%, the optimum mode is the continuous mode. However, batch mode is the optimum if the PV penetration greater than

40%. In batch mode, 85% PV penetration has the lowest LCOE and LCOW. Among the five locations were studied, Haddar is the best location from performance and cost point of view. In general, the breakeven point of fuel price, where using PV becomes feasible, is \$0.58 per liter.

ملخص الرسالة

الاسم الكامل: عبد المجيد خالد علي الربيعان

عنوان الرسالة: تحليلات الكفاءة والتكلفة لأنظمة تناضح عكسي مصغرة لمياه قليلة الملوحة تستمد طاقتها من نظام هجين (ديزل/كهروضوئي)

التخصص: الهندسة الميكانيكية

تاريخ الدرجة العلمية: ديسمبر 2018

العديد من الآبار في السعودية لا يمكن الاستفادة منها مباشرة بسبب ملوحتها العالية. الهدف من هذه الدراسة هو إيجاد أفضل نظام تناضح عكسي مزود بنظام طاقة هجين (ديزل/كهروضوئي) لتحلية مياه آبار ذات ملوحة 6000 جزء من مليون لخمس مناطق في السعودية: أمّالج، وبريدة، وهذّار، والقرية العليا، وسحمة. كل نظام تناضح عكسي يقوم بتحلية 202 متر مكعب يوميا لهدفين: الشرب، والاستخدامات المنزلية الأخرى. تم دراسة نوعين من الأنظمة: النظام المؤقت وهو النظام الذي يعمل 5 ساعات يوميا، والنظام المستمر الذي يعمل طوال ساعات اليوم واللييلة. في كل نوع، تم دراسة فائدة إضافة خزان ماء ثانٍ للاستخدامات المنزلية، وفائدة إضافة مرحلة تحلية ثانية، وتأثير استخدام مبادل الضغط على النتائج. كما تم تحليل تأثير سعر الوقود على النظام. تم تصميم النظام ومحاكاته باستخدام برنامج (ROSA) وبرنامج (HOMER). أظهرت النتائج أن إضافة خزان ماء ثانٍ للاستخدامات المنزلية بملوحة 1000 جزء من مليون سيقّل تكلفة الماء المنتج بحوالي 11%. أيضا، استخدام مبادل الضغط سيقّل من استهلاك النظام للطاقة بنسبة 26%، بينما إضافة مرحلة تحلية ثانية يقلّلها بنسبة 22%. لكن، من الناحية الاقتصادية فإنه إضافة مبادل ضغط يكون مجدي في النظام المستمر فقط. أظهرت النتائج أيضا أن أفضل تصميم لوحدة التناضح العكسي هو النظام ذو المرحلتين. فيما يتعلق بالطاقة، فإن كانت نسبة مشاركة النظام الكهروضوئي أقل من 40% فإن النظام المستمر هو الأفضل. بينما يكون النظام المؤقت أفضل عندما تكون نسبة مشاركة النظام الكهروضوئي أكثر من 40%. في النظام المؤقت، 85% هي أفضل نسبة مشاركة للنظام الكهروضوئي. من بين الخمس مناطق التي تم دراستها، هذّار هي الأفضل من ناحية تقنية واقتصادية. بشكل عام، نقطة التعادل لسعر الوقود (التي يكون عندها استخدام النظام الكهروضوئي مجديا) هي 0.58 دولار لكل لتر. |

Chapter 1: Introduction

1.1. Introduction:

In this thesis, performance and cost analyses conducted to investigate the optimal Reverse Osmosis (RO) system powered by two energy sources: Diesel Generator (Gen) and Photo-Voltaic (PV) modules for five remote areas in the Kingdom of Saudi Arabia (KSA). This chapter introduces the basics of water resources and categories, desalinations systems, power sources used in this study and thesis motivation, objectives and methodology.

1.2. Water Resources and Categories:

Water resources study is one of the important research areas nowadays. Despite water is covering 70% of our planet, but most of it is not suitable for daily use. In details, only 2.5% of earth water is fresh water while the remaining is seawater. In addition, 80% of the fresh water is found in the form of ice or soil moisture. Only 0.5% of our planet water is suitable for direct use. It is accumulated mainly in rivers, lakes and ground water. Furthermore, this 0.5% is not evenly

distributed around the globe [1]. Figure 1 illustrates the percentage of each water resources types.

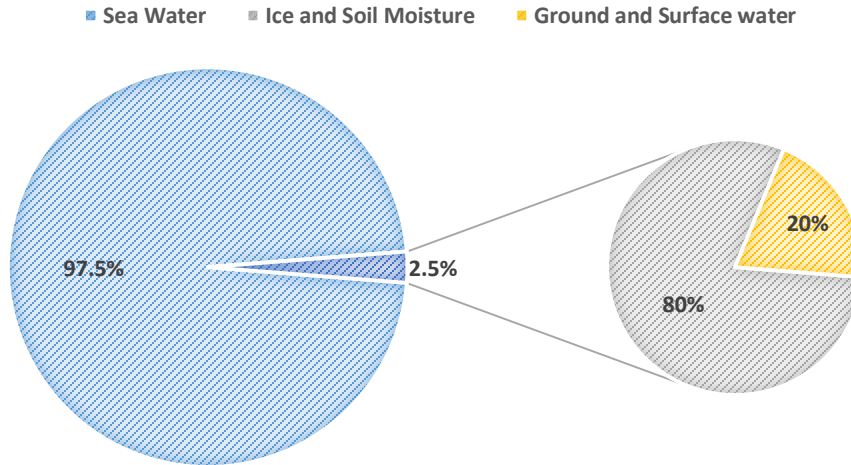


Figure 1. Water Resources Allocation

Water stress index represents the availability of water in countries. It is the ratio of the total water consumption to the renewable water supply.

Figure 2 shows the water index for world countries in 2015. It shows that Saudi Arabia has high index.

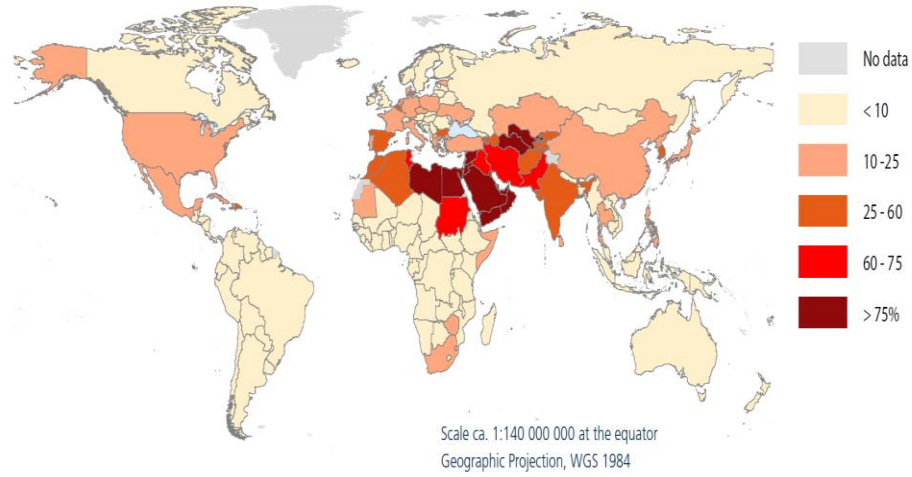


Figure 2. Water Stress Index in 2015 [2]

To gain a better understanding of available water resources, Table 1 describes in details the water resources distribution around the world. In Saudi Arabia, the major resources are the desalinated seawater and the aquifers water, which is our focus in this study. In 2017, 69% of the used water came from the seawater desalination plants, where 31% came from the wells [3].

Water can be divided according to many aspects, one of those is the salinity in part per million (*ppm*) unit. Each application has a salinity range as demonstrated in Table 2.

Table 1. Water Resources Distribution [4]

Resource	Volume (km^3)	Percent of Total Water (%)	Percent of Fresh Water (%)
Atmospheric Water	12900	0.001	0.01
Glaciers	24064000	1.72	68.7
Ground Ice	300000	0.021	0.86
Rivers	2120	0.0002	0.006
Lakes	176400	0.013	0.26
Marshes	11470	0.0008	0.03
Soil Moisture	16500	0.0012	0.05
Aquifers	10530000	0.75	30.1
Lithosphere	23400000	1.68	-
Oceans	1338000000	95.81	-
Total	1396513390	100	100

Table 2. Water Categories [4]

Salinity (ppm)	Applications	Sources	Classification
Less than 150	Drinking water	Rivers, Lakes	Fresh Water
150 – 1000	Household purposes, some industrial applications	Industrial desalination processes	
1000 - 3000	irrigation purposes, industrial cooling	Ground water	Brackish water
3000 – 35,000	-	Underground water	Brackish water
35,000 – 45,000	-	Sea and Oceans	Sea water

1.3. Water Demand:

As the population increases, the need for fresh water increases as well. In general, the average per capita consumption for drinking water is 2 *Liters/day* while the rate for others household purpose, such as cooking and washing, is 200-400 *Liters/day* [4]. In Saudi Arabia, the per capita consumption for household applications is 265 *Liters/day*. The highest region from consumption point of view is the eastern region with average per capita of 364 *Liters/day*. Figure 3 demonstrates the average per capita consumption for different Saudi regions. For last five years, the water demand raised 5% every year. [3]

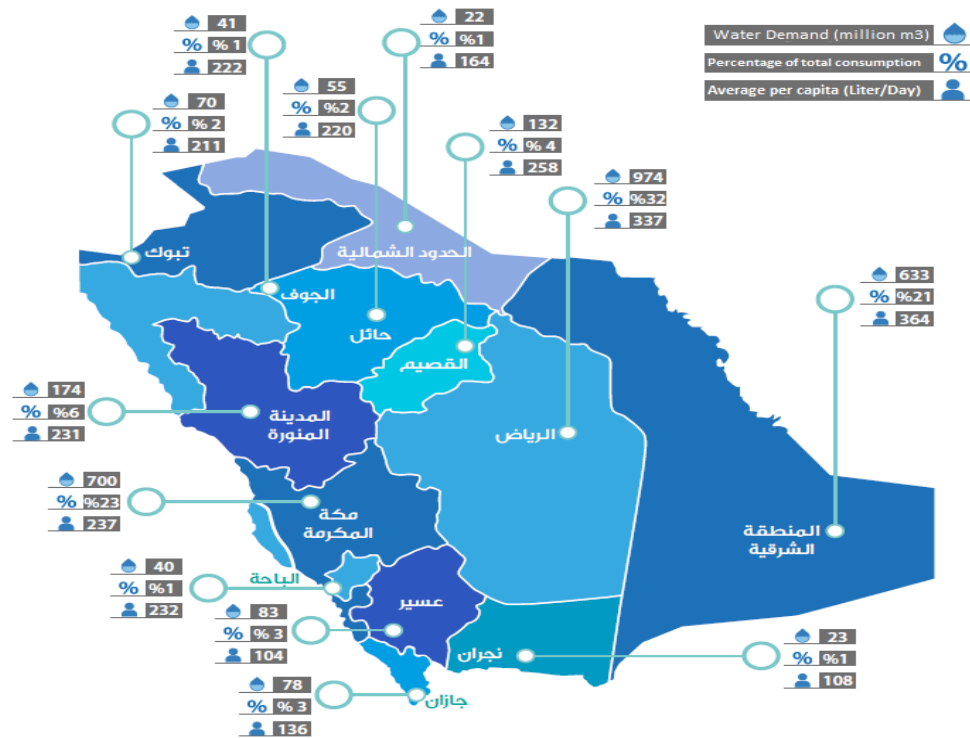


Figure 3. The water consumption in KSA in 2015 [3]

1.4. Desalination Definition and Methods:

Desalination came from the root "desalt" which mean to "eliminate salt from". In industry, desalination is the process to separate dissolved solids from water. Dissolved solids can be salt or other minerals [1].

Generally, desalination methods can be divided into two main categories. First, the thermal desalination that depends mainly on evaporation and condensation. A Solar still is one of the basic idea in this category. It represents the natural water cycle but in controlled environment. In addition, humidification-dehumidification method (HDH) is the process of wetting air by passing it through sprayed water in humidification section. Then, condensation of the moisture occurs in the dehumidification section. For large scale production, the multistage flash desalination (MSF) and the multiple effect evaporation (MEE) are the most effective and reliable thermal methods.

Second, the membrane desalination that depends mainly on some sort of semi-permeable membranes to separate the fresh water from the brine. Reverse Osmosis (RO) and Electrodialysis (ED) are the main methods under this category. The classification of common desalination methods is shown in Figure4 [4].

In KSA, the daily production from all desalination plants during 2017 was 7,653,143 cubic meter while the total water desalinated in 2017 was 2,458 million

cubic meter. Generally, 46% of plants is MSF plants while 38% and 16% is RO and MED respectively [3].

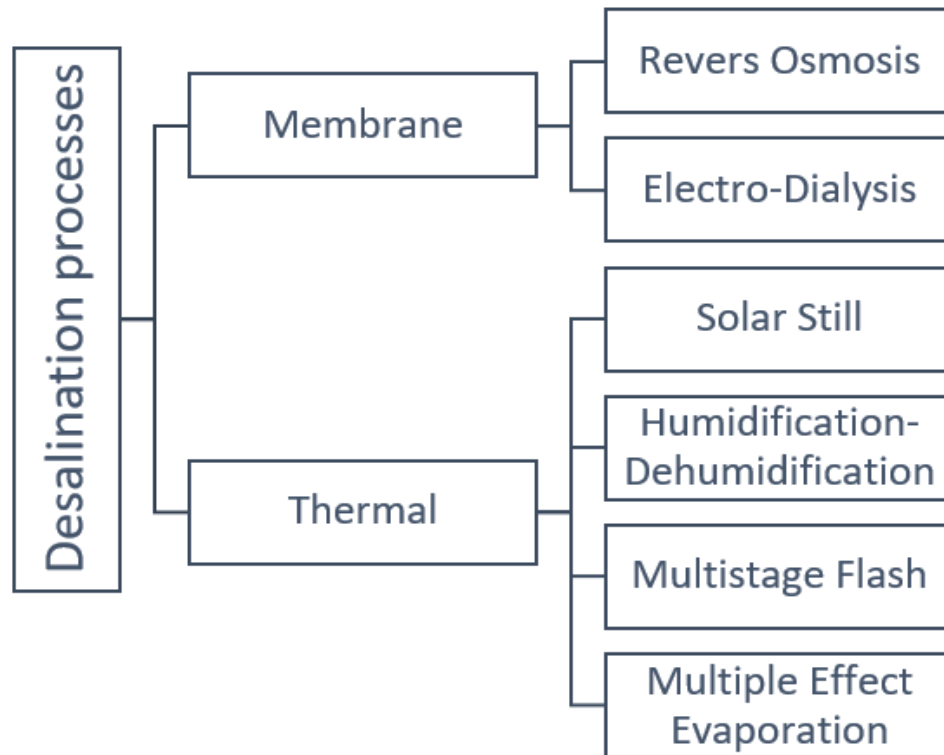


Figure4 . Classification of Common Desalination Processes

1.4.1. Reverse Osmosis Desalination System:

Osmosis is a natural phenomenon that occurs when a semipermeable membrane separates two solutions. The solvent of the lower salinity solution tends to pass through the membrane faster than its solid particles until the salinity between the two solutions balance. Generally, the direction of flow is from the

higher chemical potential solution to the lower one. The chemical potential of a fluid is a function of its pressure, temperature and the dissolved particles concentration.

In Reverse Osmosis (RO), an external pressure is applied on the higher salinity side to increase its chemical potential. When the chemical potential increases more than the other side, the direction of flow reversed as illustrated in Figure 5.

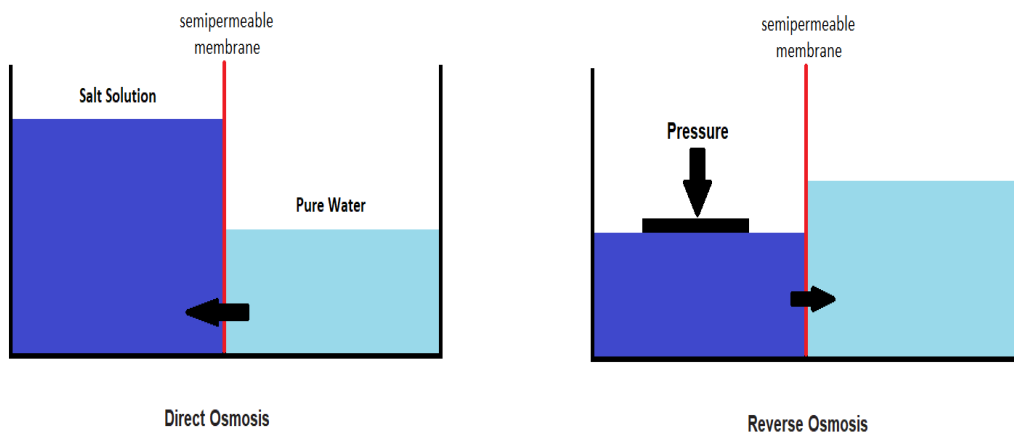


Figure 5. Direct and Reverse Osmosis Process

The basic components of RO desalination system are:

1. Feed water supply unit;
2. Pre-treatment system;
3. High pressure pumping unit;

4. Assembly unit for membrane element;
5. Control system;
6. Electric power supply system;
7. Post-treatment; and
8. Storage unit.

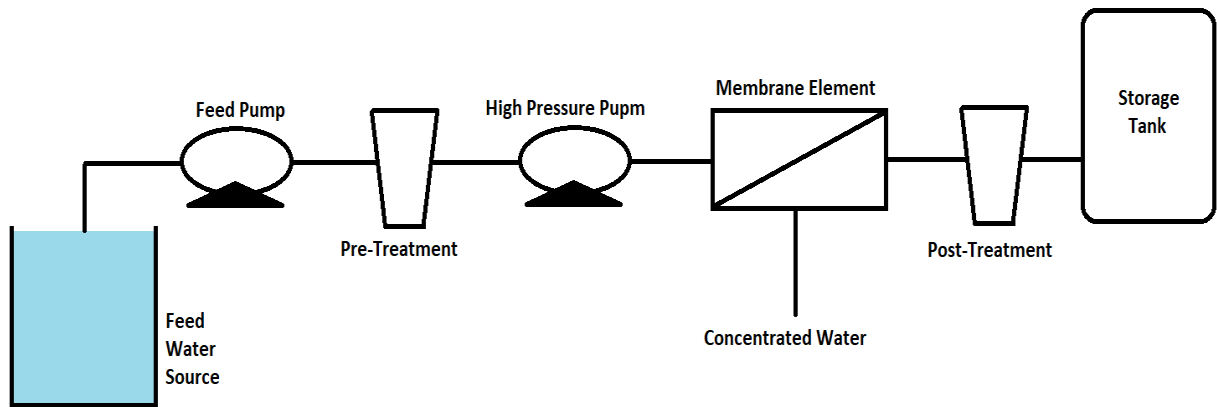


Figure 6. Basic Components of RO System

The heart of the RO system is the high-pressure pump, which forces the water to permeate through the membrane. Water coming to the membrane is called feed water. After the membrane, this feed water is divided into two portions, permeate water with low salinity and concentrated water with high salinity. The permeate water is the desalinated water while the concentrate water is the brine.

The feed water goes through pre-treatment filters before the membranes to eliminate particles with relatively large size and any materials that may affect the membrane. This process increases the life and efficiency of the system by minimizing the scaling, fouling and membrane degradation. After the membrane,

the permeate water goes through post-treatment process. In this process, chemicals are added to the desalinated water to become suitable for the needs.

[5]

The membrane has various types available in the market. Now a day, the most common type of membrane element is the Spiral Wound element, which describes in

Figure 7. In RO plant, number of membrane elements connected together in series and inserted inside a pressure vessel, which hold the membrane in high-pressure water flow. RO systems can be defined based on the type of connection between the pressure vessels. If the concentrated water (brine) re-desalinate in another pressure vessel, this system is called RO with two stages. However, If the permeate water re-desalinate in another pressure vessel, this is called RO system with two passes. Table 3 summarizes the important RO parameters, its definitions, its correlations and some notes [1].

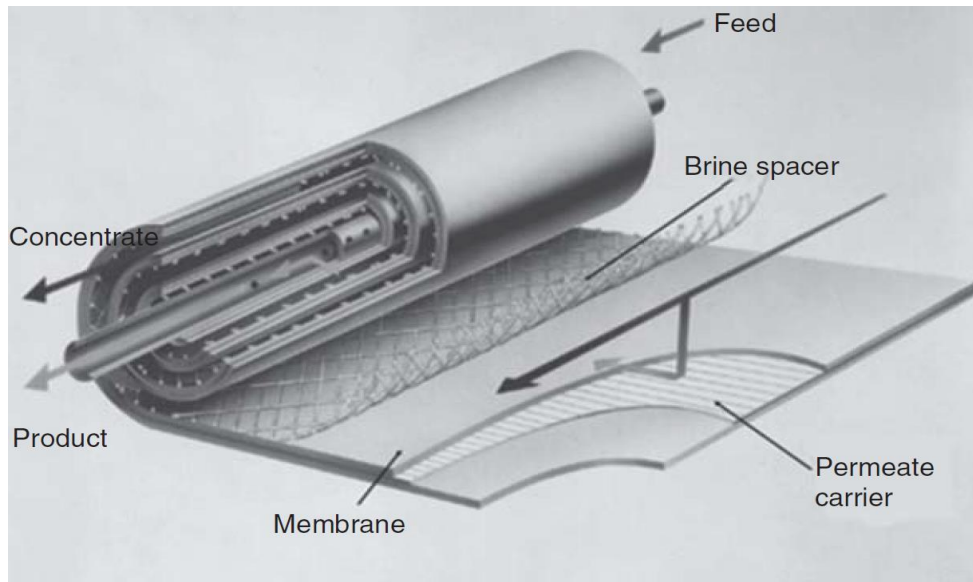


Figure 7. Configuration of Spiral Wound Membrane Element [1]

Table 3. Summary of RO parameters [1]

Parameter	Definition	Correlation	Notes
Osmotic Pressure (P_{osm})		$P_{osm} = R(T + 273) \sum m_i$	R is the universal gas constant T is the temperature (in °C) $\sum m_i$ is the molar concentration of all element in the solution
Permeate recovery Rate (R)	Conversion Ratio	$R = 100\% \left(\frac{Q_p}{Q_f} \right)$ <p>Or</p> $R = 100\% \left(\frac{Q_p}{Q_p + Q_c} \right)$	Q_p is the product water flow rate Q_f is the feed water flow rate Q_c is the concentrate (brine) water flow rate

Net Driving Pressure (NDP)	Is the net pressure that drive the water to flow through the membrane	$NDP = P_f - P_{os} - P_p - 0.5P_d (+P_{osp})$	<p>P_f is the feed pressure</p> <p>P_{os} is the average feed osmotic pressure</p> <p>P_p is the permeate pressure</p> <p>P_d is the pressure drop across the membrane</p> <p>P_{osp} is the osmotic pressure for permeate</p>
Water Transport (Q_w)	Is the water flow rate through the membrane	$Q_w = (\Delta P - \Delta P_{osm}) K_w \left(\frac{S}{d} \right)$ <p>Or</p> $Q_w = A S NDP$	<p>ΔP is the hydraulic pressure difference across the membrane</p> <p>ΔP_{osm} is the osmotic pressure difference across the membrane</p> <p>K_w is the water membrane permeability coefficient</p> <p>S is the membrane area</p> <p>d is the membrane thickness</p> <p>A is the water transport coefficient</p> <p>Unit: $\frac{g}{cm^2-sec}$</p>
Salt Transport (Q_s)	Is the salt flow rate through the membrane	$Q_s = (\Delta C) K_s \left(\frac{S}{d} \right)$ <p>Or</p> $Q_s = B S \Delta C$	<p>ΔC is the salt concentration difference across the membrane</p> <p>K_s is the salt membrane permeability coefficient</p> <p>B is the salt transport coefficient</p> <p>Unit: $\frac{cm}{sec}$</p>
Salinity of permeate (C_p)	Is the ratio between salt transport to water transport	$C_p = \frac{Q_s}{Q_w}$	

Salt Passage (SP)	Is the ratio between the salt concentration in the permeate side to the average salt concentration in the feed side	$SP = 100\% \left(\frac{C_p}{C_{fm}} \right)$	C_{fm} is average salt concentration in the feed side
Salt Rejection (SR)		$SR = 100\% - SP$	
Temperature Correction Factor (TCF)	The flow rate through the RO membrane affected by the temperature	$TCF = \frac{1}{e^{C \left(\frac{1}{273+t} - \frac{1}{298} \right)}}$	t is temperature C is a constant depends on membrane barrier material
Average Permeate Flux (APF)	Is the permeate flux divide by the total membrane area in the RO system	$APF = \frac{Q_p}{EN \ MA}$	EN is the number of elements in the system MA is the membrane area per element
Specific Flux (SF)	Is a membrane material characterization in term of water flux rate driven by the net driving pressure gradient	$SF = \frac{APF}{NDP}$	APF is the average permeate flux NDP is the net deriving pressure

1.5. Power Sources:

Generally, power sources can be divided to two main categories. First, a traditional power source, which depends on the traditional energy sources such as diesel. Second, renewable power source, which depends on the renewable energy sources. Renewable energy is the type of energy where its source does not has a limited quantity. In other words, the resources inputs are more than or equal

the outputs. For instant, sun is one source of renewable energy. Solar energy can be used either directly by heating or converting it to electricity through the photovoltaic effect. In this study, three types of power sources are used: Diesel Generator (Gen), Photovoltaic Panels (PV) and Electric Batteries.

1.5.1. Diesel Generator:

Diesel Generator is a device that converts chemical energy to electrical energy. This conversion process has three main steps. First, the chemical energy converts to thermal energy by burning the fuel. Second, the thermal energy converts to mechanical energy using turbines. Third, the mechanical energy converts to electrical energy through the electro-magnetic effect.

1.5.2. Photovoltaic Cells:

It is a semiconductor materials, usually silicon, have a photo-voltaic (PV) phenomena which converts the light directly to electricity. PV module consists of many PV cells connect to each other in parallel or series manner. The voltage of the cell depends mainly on the cell temperature while the current depends mainly on the solar irradiance. The cell that has higher temperature would have lower voltage output, while the cell that receives more irradiance would produce more

current. The total power output from the cell is the multiplication of voltage and current.

This type of power source is free of Greenhouse Emissions, which have bad effects on the atmosphere, which increase the global warming problem.

1.5.3. Electrical Batteries:

This type of power source is used to store the electrical energy in the form of chemical reactions. Since the solar energy is available only in the daytime with fluctuating amount, storing the energy is very important. Lead Acid and Lithium Ion Batteries are the most common battery types in renewable energy applications.

1.5.4. Energy Recovery Devices (ERD):

In RO systems, large amount of the energy is lost as pressure in the concentrated water. To make use of this lost energy, energy recovery devices are used. There are many types of ERD used for RO system in the industry such as Pelton Wheel, Turbocharger and Pressure Exchanger (PX). PX is a device that transfers the mechanical energy (in form of pressure) from high pressure flow to low pressure flow. Figure 8 shows PX components.

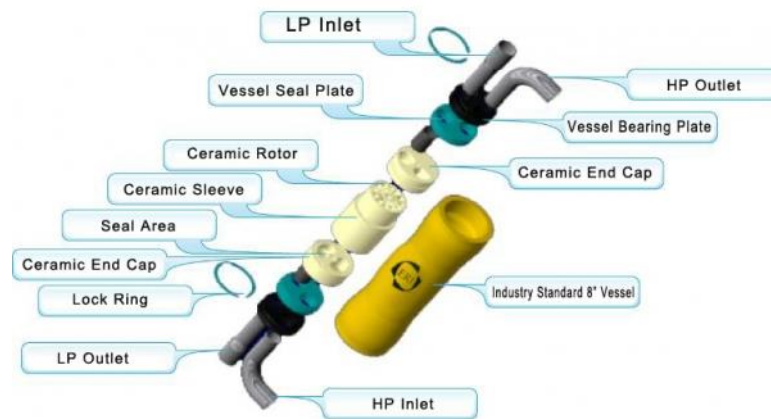


Figure 8. Pressure Exchanger Components [6]

1.6. Motivations:

The motivations of selecting this topic are:

- Finding a sustainable water resource for remote areas with good quality.
- Reducing our dependence on sea water desalination.
- Managing our energy resources in an efficient way.
- Saving our environment from the harmful gases.

1.7. Objectives:

The main objective of this thesis is to analyse the performance and cost of a hybrid diesel-PV powered RO system to desalinate brackish well water for five remote areas in Saudi. The specific objectives for this study are:

- Building a model to evaluate the design and operation of hybrid diesel-PV RO system.
- Studying the feasibility of using small RO units powered by PV modules or PV with diesel generator to desalinate a brackish water for remote areas in Saudi Arabia.
- Studying the optimum RO operation mode to integrate it with PV system.
- Studying different RO configurations to find the optimum one.
- Analyzing the effect of adding PX as ERD to BW-RO systems.
- Analyzing the important techno-economic parameters in the system and recommending the best design and operation characteristics for remote areas in KSA.

1.8. Methodology:

The work starts by selecting the location where the RO system is studied. This selection is based on the aimed water salinity and daily feed flow rate

capability for a remote area. Then, collecting all information about the weather conditions, water properties and the location needs. After that, a RO system will be modeled using Reverse Osmosis System Analysis software (ROSA) and other equations to simulate the ERD and new configurations. Then, different scenarios are studied to find the best scenarios. In addition, validation will be performed. After identifying the load required for the RO system, a power system is modeled using Hybrid Optimization of Multiple Energy Resources software (HOMER). Different scenarios are studied to figure out the best scenarios. Next step is to match the best model for both power and RO systems and to apply it for four more locations with same feed salinity and different environmental resources.

Chapter 2: Literature Review

2.1. Introduction:

During last years, there are lots of researches and projects in the field of desalination plants powered by renewable energy. RO system is the most attractive one due to its low energy consumption in comparison with others desalination methods. On the other hand, solar PV technology price decreases gradually last ten years. Thus, many works tried to study, evaluate and improve RO plants powered by PV modules. These researches can be divide into three main sections from purpose point of view: reliability and performance studies, effect of parameters studies and techno-economic studies. Finally, summary of some previous works lists in Table 4.

2.2. Reliability and Performance Studies:

Some studies aim to show the reliability and performance of PV-RO system either by experimental or modeling works.

In 1995, Alawaji et al. [7] built a PV-RO plant for remote area in Saudi Arabia to desalinate a brackish water for drinking purpose. The plant production

was 15 m^3 per day where the PV size was 10 kW with battery. Further work conducted in 1996 by making two options: battery and battery less [8]. They state that the performance of the plant was excellent and the system was reliable. PV modules cost 42% of the total investment, while 31% for batteries and charge controller.

Another PV-RO setup evaluation was in Brazil on 2009. Riffela and Carvalho [9] compared two scenarios. First scenario, 2 PV modules used to operate RO pump and 1 module for well pump. Second scenario, all 3 modules used for both loads. The study shows that the second scenario was the best.

In 2015, Elasaad et al. [10] evaluated a PV-RO setup in a remote area in Mexico, which was operating for 6 years. The setup desalinate wells water with 1 m^3 per day production rate and 800 W power generation. The study shows that one cubic meter of desalinated water cost \$9. Half of the capital cost was for the RO system, pretreatment and posttreatment while 25% was for the PV modules and electronics. Regarding the operating cost, 61.5% was for the operators salaries and 9.23% for RO maintenance. The system is efficient and reliable.

Another paper in 2015 compared between electro dialysis reversal (EDR) and RO systems integrated with PV modules. Karimi et al. [11] states that for low salinity water, PV-EDR is more efficient than PV-RO while for high salinity water is the opposite.

Peñate et al. [12] reported their experience with a PV-RO plant in Tunisia for 7 years of operation. The plant production rate is 50 m^3 per day with 10.5 kW PV power generation. The plant has an electrical storage system. A successful uninterrupted operation has been reported.

2.3. Effect of Parameters Studies:

The goal of some studies is to investigate the effect of some parameters on the system either for RO side or for PV side.

In Jordan during 2005, Abdallah et al. [13] evaluated a PV-RO setup and investigated the effect of tracking system on setup performance. The water production increased by 15% when they used east-west one axis tracking system compared with fixed axis system while the electric production raised 25 %.

In 2011, Poovanaesvaran et al. [14] discuss the design parameters for a successful small scale PV-RO system for brackish water applications. They state that the small scale desalination plant is the plant that has a water production rate less than 60 m^3 per day. In summary, to build a good small PV-RO system, minimized the cost of fresh water. The most important cost variable is the energy. Using energy recovery device will reduce the cost of water production. Also, they discuss the effects of water characteristic, fouling and scaling, pre-treatment, reject water management and RO design configurations. The arrangement of RO

modules should be determined by the feed water salinity and the quality of water production. If the recovery ratio of water is less than 50% for single stage, two-pass system is more efficient.

In the same year, Bilton et al. [15] presented a general method to evaluate PV-BWRO system feasibility for small and remote area. The feasibility study is done by comparing the cost of producing water by RO system with the cost of water produced by conventional diesel system. For PV-RO, the cost mainly depends on the location due to differences in solar irradiance, water quality, demand of the system and the government policies. This study demonstrates that PV-RO system is feasible for most of the remote places with high solar resources. It shows the cost of water desalinated by PV-RO system in the Middle East. This study states that the cost of water desalinated by PV-RO is less than the cost of water desalinated by diesel for Jeddah, without the government subsidies.

Clarke et al. [16] modeled a PV-RO system using MATLAB software. This paper shows how to simulate a small-scale stand-alone PV-RO system and investigates the effects of different parameter on the system for two cases: battery and battery-less.

For different latitudes, Poovanaesvaran et al. [17] found that two stages RO system is the best, for small-scale brackish water plant, with lower energy consumption. The system produces 60 m^3 daily while the PV size is 28 kW with battery.

In India in 2015, Kumarasamy et al. [18] studied the effect of storage tank on the water production rate. They compared two RO plants: with storage tank and without. They concluded that it is better to have storage tank in the RO desalination plant.

Richards et al. [19] studied the effect of solar irradiance on the RO performance. They show that for irradiance from 400 until 1200 *per m²*, the RO performance seems to be stable. But, for irradiance below 300 Watt per *m²* the permeate flux becomes low and the NaCl concentration becomes high.

Ahmad et al. [20] studied the effect of PV tilt angle and the tracking system in the performance of RO system. Modeling, simulation and experimental work reveal that the optimal yearly PV tilt angle is 0.913 times latitude of Dhahran city. Also, they suggest to adjust PV orientation using single or dual axis tracking systems.

In 2016, Raval and Maiti [21] presented a novel idea to reduce the SEC by 40%. The idea is cooling the PV module by the feed water and modifying the membrane morphology toward more hydrophilicity.

2.4. Techno-economic Studies:

After knowing the reliability of the PV-RO system and the parameters effect on the performance of the system, researchers did many techno-economic studies to match between the best PV-RO output and the lowest cost.

In 2002, Thomson and Infield [22] analyzed the cost and performance of PV-RO system in Eritrea. This system assumed to be a battery less system which desalinate a sea water with 40,000 *ppm* salt concentration to become 1,000 *ppm*. The size of PV array is 2.4 *kW* while the daily production rate is 3 m^3 . MATLAB software is used to model the system. They assumed the system life to be 20 years with pump replacements every 5 years, RO elements change every year and 8% discount rate. The results show that the system will cost £2 per m^3 while the SEC is greater than 10 *h per m³*. Thomson and Infield [22] state that to get SEC less than 10 *kWh per m³* the feed water should be brackish water (less than 10,000 *ppm*).

In the same year, Ahmad and Schmid [23] performed a cost analysis of PV-RO system for Egypt desert conditions. The feed is a brackish water and the production rate is 1 m^3 per day. The size of PV is 1.1 *kW* with battery for stability purpose. They assumed 7 hours operation per day. RO and battery replacement every 5 years. The outcome was \$3.73 per m^3 .

Helal et al. [24] studied the economical feasibility of three RO systems scenarios in UAE. The difference between those scenarios is the power source. Diesel generator, hybrid diesel-PV and PV panels are the different power sources. The system desalinates the sea water with production rate of 20 m^3 per day. The cost and energy consumption for one meter cube of water are \$7.64 and 7.74 *kWh* for diesel scenario, \$7.21 and 7.73 *kWh* for hybrid scenario and \$7.34 and 7.33 *kWh* for PV scenario.

In 2014, Zeiner et al. [25] performed a techno-economic analysis of PV-RO setup to desalinate a brackish water in Paraguay. PV modules have a power of 319 *kW* and the RO system produces 255 m^3 per day. They compared two cases. In the first case, the system operates 24 h a day at a constant rate. For the second case, the production rate is reduced to half in the nighttime. This study demonstrates that the second option is the best because the cost reduction due to lower battery storage size is more than the cost of larger membrane.

In the same year, Zeiner et al. [26] also studied the cost analysis of RO system operating, partially, by PV modules in Paraguay.

Bilton and Kelley [27] developed an approach based on optimization techniques to choose the best power sources, RO configurations and appropriate capacity of water storage for remote communities. This method consider diesel generators, solar PV, wind and their combinations. In addition, this approach is applied on three different locations: Honduras, Eritrea and Australia.

Garg and Joshi [28] optimized and economically analyzed a small PV-RO system with adding a Nano-filtration (NF) membrane. They compared three scenarios: single RO system, single NF system and hybrid NF/RO system with different configurations. The results show that the most efficient system was the hybrid NF/RO system with highest recovery rate and lowest specific energy consumption (SEC). The performance is affected by many factors, such as NF/RO integration mode, recovery ratio, daily average operating hours and the subsidies.

In Egypt, Zaid [29] examined two different modes for a PV-RO system to desalinate a seawater for the purpose of conducting a techno-economic analysis. The first mode is a daytime mode with 3.5 m^3 per day production rate and average cost of 7.5 LE (LE during 2012). The second mode is night mode with 12.2 m^3 per day production rate and average cost of 2 LE.

In Malaysia, Alghoul et al. [30] designed and tested a PV-RO small setup to desalinate water from salinity of 2000 *ppm* to less than 50 *ppm*. They show that under Malaysia climate condition, 2 *kW* PV can only power 600 *W* of RO load. When the system operates for 10 *h*, the water production is 5.1 m^3 at SEC of 1.1 *kWh per m*³.

Another PV-RO setup evaluation was conducted in Tanzania. Shen et al. [31] compares 4 RO types integrated with Nano-filtration. For the best type, the production rate was 1582 Liter per day while the specific energy consumption was 1.6 *kWh per m*³. The main concern in this paper is the concentration of Fluoride.

In 2015, Fthenakis et al. [32] used HOMER software to do a techno-economic analysis of RO-PV systems that desalinate a sea water. The first phase of their work was a comparison between a dual axis concentrated photo-voltaic (CPV) equipped with triple junction III/V cells and a CdTe PV cells. The cost of CPV was \$0.16 per kWh while the cost of CdTe PV was \$0.1 per kWh for fixed tilt angle and \$0.09 per kWh for one axis tracking system. In the second phase, they used the CdTe PV in two scenarios: small RO system and large RO system. For small RO scenario with fixed tilt angle at the latitude, the water cost was \$1.39 per m^3 . For large RO scenario with one axis tracking, the water cost was \$0.85 per m^3 .

Jones et al. [33] investigated the performance and cost analysis of PV-RO system used for agriculture applications in three different location at Jordan Valley. The feed water is wells water. PV array size range from 50 up to 65 kW . The water cost per cubic meter is between \$0.83 and \$1.23. Furthermore, they compared the RO system powered by PV with RO system powered by diesel generator and RO system powered by the electrical grid. The best choice from economic point of view was the grid choice followed by PV choice then the diesel choice, for the assumed prices.

In Iran, Esfahani and Yoo [34] introduced a method to optimize the best PV-RO arrangements and performance. They modeled 92 PV modules and 11 RO elements to produce 10 m^3 per day. The water cost of this desalination plant is

\$13,652 per year. They used water storage tank to perform reliability instead of batteries.

In conclusion, since there are studies that showed some benefits of using hybrid power system to operate RO plant in another part of the world, it would be a motivating factor to study the feasibility of such systems in KSA. In addition, the techno-economic study for RO system powered by hybrid diesel-PV for remote area in KSA is a new study.

Table 4 Summary of some previous works

Ref No.	Date	Location		PV Size (kW)	Adj. RO Size ($\frac{m^3}{d}$)	Cost	Adj. Cost ($\frac{\$}{m^3}$)	SEC ($\frac{kWh}{m^3}$)	Mode	Feed Water
[22]	2002	Eritrea		2.4	3	$2 \frac{\pounds}{m^3}$	3.14	>10	batteryless	SW
[23]	2002	Egypt		1.1	1	3.73	3.73	-	battery	BW
[24]	2008	UAE		-	20	Diesel	7.64	7.74	Batteryless	SW
						Hybrid	7.21	7.73		
						PV	7.34	7.33		
[9]	2009	Brazil		0.165	0.26	-	-	1.57	batteryless	BW
[28]	2014	India	RO +NF	1.5	0.93412	$99.81 \frac{RS.}{m^3}$	1.64	5.02	Batteryless	BW
			NF		0.51991	158.46	2.6	9.35		
			RO		0.20571	400.5	6.57	17.6		
			RO +NF		0.93412	133.88	2.2	5.02	battery	
			NF		0.51991	219.63	3.6	9.35		
			RO		0.20571	555	9.1	17.6		

[29]	2015	Egypt	-	3.5	$5.6-9.3 \frac{LE}{m^3}$	0.9-1.55	-	Batteryless	SW
			-	12.2	$1.7-2.3 \frac{LE}{m^3}$	0.28-0.38	-	battery	
[10]	2015	Mexico	0.8	1	9	9	-	-	-
[34]	2016	Iran		10	$13,652 \frac{\$}{year}$	3.74	-	batteryless	
[33]	2016	Jordan	50-65	-	0.83 - 1.23	0.83 - 1.23	-	batteryless	BW to agriculture

Chapter 3:

Mathematical Model and Validation

3.1. Introduction:

In this chapter, the mathematical equations to simulate the reverse osmosis system powered by hybrid diesel-photovoltaic are introduced. Equations can be divided into 4 categories. First, Energy/Power equations, which demonstrate the relation between energy source and electrical power in the system. Second, Power/Pressure equations, which present how the desired pressure is produced to desalinate water through the membrane. Third, Pressure/RO equations, which explain the flow rate, salinity and pressure before and after the membrane. Finally, the economic equations. In addition, validation of the model is performed.

3.2. Mathematical model:

The governing equations for hybrid diesel-PV powered RO system are based on two fundamental laws: mass conservation and energy conservation. Most of the equations in this chapter are derived from either the continuity equation or the energy equation.

3.2.1. Energy/Power Equations:

In this study, there are three types of power sources: Photo-Voltaic Panels, batteries and diesel generator. The rated power equation for PV is [15]:

$$P_{PV-rated} = \eta_{PV} A_{PV} G_{STC} \quad (3.1)$$

Where,

$P_{PV-rated}$ is the rated power generated by the solar panel (W)

η_{PV} is the panel efficiency.

A_{PV} is the panel area (m^2).

G_{STC} is the incident solar energy at the standard test condition
($\frac{W}{m^2}$).

The standard test condition (STC) for PV module means three numbers: $1000 \frac{W}{m^2}$ solar irradiance, $25^\circ C$ cell temperature and 1.5 mass density. The real power output from the solar panel, at real conditions, can be calculated using the following equation [35]:

$$P_{PV-output} = P_{PV-rated} F_{PV} \left(\frac{G}{G_{STC}} \right) [1 + \alpha_p (T_{cell} - T_{cell-STC})] \quad (3.2)$$

Where,

- $P_{PV-output}$ is the real power generated by the solar panel (W)
- F_{PV} is the derating factor which account for the loss due to wiring, shading, snow and etc.
- G is the incident solar energy on the panel ($\frac{W}{m^2}$).
- α_p is the cell temperature coefficient ($\frac{\%}{^\circ C}$).
- T_{cell} is the cell temperature ($^\circ C$)
- $T_{cell-STC}$ is the cell temperature at standard test condition ($^\circ C$)

The second power source is the electrical batteries. The governing equation for battery power is [10]:

$$\frac{dE_B}{dt} = P_{PV} - P_{out} \quad (3.3)$$

Where,

$\frac{dE_B}{dt}$ is the rate of change of energy stored in the batteries (W).

P_{out} is the output power (W).

The third source is the electrical generator. The rate of used diesel fuel is given as [15]:

$$\dot{m}_{fuel} = \frac{P_{needed}}{\eta_{Gen} \Delta H^0_{comb}} \quad (3.4)$$

Where,

\dot{m}_{fuel} is the fuel used rate ($\frac{kg}{s}$).

P_{needed} is the total power needed in the system (W).

η_{Gen} is the generator efficiency.

ΔH^0_{comb} is the diesel fuel net calorific value ($\frac{J}{kg}$).

3.2.2. Power/Pressure Equations:

After converting the energy to power, pumps are used to convert the power to pressure. The main pump in the system is the high-pressure pump, which can be calculated as follow [15]:

$$P_{HP} = 27.78 \frac{Q_f p_f}{\eta_{HP}} \quad (3.5)$$

Where,

P_{HP} is the power of high pressure pump (W).

Q_f is the feed flow rate ($\frac{m^3}{h}$).

p_f is the feed pressure (bar).

η_{HP} is the motor and pump efficiency.

The constant (27.78) is the unit conversion factor. It converts (bar) to (Pa)

and ($\frac{m^3}{h}$) to ($\frac{m^3}{s}$).

For the energy recovery devices, which is the pressure exchanger in this study, the power can be related to pressure as follow [15]:

$$P_{ERD} = 27.78 \eta_{ERD} Q_c p_c \quad (3.6)$$

Where,

P_{ERD} is the power of energy recovery device (W).

Q_c is the brine flow rate ($\frac{m^3}{h}$).

p_c is the brine pressure (bar).

η_{ERD} is the energy recovery device efficiency.

The constant (27.78) is the unit conversion factor.

The power required to transport water from the well to the system can be described in the following equation [15]:

$$P_{Tr} = \frac{Q_f \rho g h}{3.6 \times 10^3 \eta_{Tr}} \quad (3.7)$$

Where,

P_{Tr} is the power of transportation pump (W).

Q_f is the feed flow rate ($\frac{m^3}{h}$).

ρ is the water density ($\frac{kg}{m^3}$).

g is the gravity acceleration ($\frac{m}{s^2}$).

h is the water height change (m).

η_{Tr} is the transportation pump efficiency.

The constant (3.6×10^3) is the unit conversion factor.

The power used for the RO system can be calculated as follow [15]:

$$P_{RO} = P_{HP} - P_{ERD} \quad (3.8)$$

The total power consumption can be calculated as follow [15]:

$$P_{Total} = P_{RO} + P_{Tr} \quad (3.9)$$

Note that the power produced by PV, batteries and generator must meet the total power consumption.

The specific energy consumption (SEC) can be calculated as follow [15]:

$$SEC = \frac{P_{Total}}{Q_{pr}} \quad (3.10)$$

Where,

SEC is the specific energy consumption ($\frac{Wh}{m^3}$).

Q_{pr} is the permeate flow rate ($\frac{m^3}{h}$).

3.2.3. Pressure/RO Equations:

The equations (from 3.11 to 3.25) that describe the relation between pressure and the RO process are listed below [33]:

$$Q_f = Q_{pr} + Q_c \quad (3.11)$$

Where,

Q_f, Q_{pr} and Q_c is the flow rate of feed, permeate and concentrated water respectively ($\frac{m^3}{h}$).

$$Q_f C_f = Q_{pr} C_{pr} + Q_c C_c \quad (3.12)$$

Where,

C_f, C_{pr} and C_c is the salinity of feed, permeate and concentrated water respectively (*ppm*).

$$RR = \frac{Q_{pr}}{Q_f} \quad (3.13)$$

Where,

RR is the recovery ratio.

$$Q_{pr} = K A_{membrane} (TCF)(FF)(\Delta p - \Delta \pi) \quad (3.14)$$

Where,

K is the permeability coefficient ($\frac{m^3}{m^2.h.bar}$).

$A_{membrane}$ is the membrane surface area(m^2).

TCF is the temperature correction factor.

FF is the membrane fouling factor.

Δp is the average pressure differential across the membrane(*bar*).

$\Delta\pi$ is the average osmotic pressure differential across the membrane(*bar*).

$$\Delta p = p_f - \frac{\Delta p_{fc}}{2} - p_{pr} \quad (3.15)$$

$$\Delta p_{fc} = 0.01 N_E Q_{fc}^{1.7} \quad (3.16)$$

Where,

Δp_{fc} is the pressure drop from the feed to concentrate sides of a single element(*bar*).

N_E is the number of elements.

$$Q_{fc} = \frac{Q_f + Q_c}{2} \quad (3.17)$$

$$p_c = p_f - \Delta p_{fc} \quad (3.18)$$

$$\Delta\pi = p_{f_{avg}} \left(\frac{\pi_f + \pi_c}{2} \right) - \pi_{pr} \quad (3.19)$$

Where,

pf_{avg} is the concentration polarization factor.

$$C_{pr}Q_{pr} = B A_{membrane} (TCF)(pf_{avg})\left(\frac{C_f + C_c}{2}\right) \quad (3.20)$$

Where,

B is the salt diffusion coefficient ($\frac{m^3}{m^2.h}$).

$$\pi_f = \frac{C_f(T + 320)}{491000} \quad (3.21)$$

$$\pi_c = \frac{C_c(T + 320)}{491000} \quad (3.22)$$

Where,

T is the water temperature ($^{\circ}C$).

π_f, π_c is the feed and concentrated osmotic pressure (bar).

$$pf_{avg} = e^{0.7RR} \quad (3.23)$$

$$TCF = e^{3020(\frac{1}{298} - \frac{1}{273+T})} \text{ if } T < 25 \quad (3.24)$$

$$TCF = e^{2640(\frac{1}{298} - \frac{1}{273+T})} \text{ if } T > 25 \quad (3.25)$$

3.2.4. Economic Equations:

In this section, the annualized life cycle cost method is used to model the economics of the system. Cost can be divided into two main categories: capital cost and operation cost.

The aim is to find the levelized cost of desalinated water, which can be calculated using the following equation [15]:

$$LCOW = \frac{An_{total}}{365 \tau Q_{cap}} \quad (3.26)$$

Where,

$LCOW$ is the levelized cost of water ($\frac{\$}{m^3}$)

An_{total} is the total equivalent annual cost for PV and RO system (\$).

τ is the availability of RO plant (%).

Q_{cap} is the water production capability of RO plant ($\frac{m^3}{day}$).

The total equivalent annual cost is the summation of the total equivalent annual cost of the power source and RO system. These costs are modeled as follow [15]:

$$An_{total,PV} = An_{CC,PV} + An_{Op,PV} \quad (3.27)$$

$$An_{total,Gen} = An_{CC,Gen} + An_{Op,Gen} \quad (3.28)$$

$$An_{total,RO} = An_{CC,RO} + An_{Op,RO} \quad (3.29)$$

The abbreviations (*PV*) for Photo-Voltaic, (*Gen*) for Generator, (*RO*) for Reverse Osmosis, (*CC*) for Capital Cost and (*Op*) for Operation Cost.

The levelized cost of energy (LCOE) can be calculated as follow [15]:

$$LCOE = \frac{An_{total,PV} + An_{total,Gen}}{365 * P_{Total} * N_h} \quad (3.30)$$

Where,

$LCOE$ is the levelized cost of energy ($\frac{\$}{Wh}$).

P_{Total} is the total power consumption by the system (W).

N_h is the system daily operation hours (h).

The Net Present Value (NPV) can be calculated as follow [15]:

$$NPV = \frac{R_t}{(1 + i)^t} \quad (3.31)$$

Where,

i is interest rate (%).

t is the time of the cash flow.

R_t is the net cash flow at that time (\$).

The direct capital cost is converted to equivalent annual cost using the next formula [15]:

$$A_{cc} = \frac{i(1 + i)^n}{(1 + i)^n - 1} DC \quad (3.32)$$

Where,

DC is the direct capital cost (\$).

$$CC_{PV} = CC_{panel} + CC_{control\ system} + CC_{wiring} + CC_{installation} \quad (3.33)$$

$$CC_{Gen} = CC_{Generator} + CC_{installation} \quad (3.34)$$

$$CC_{RO} = CC_{pump} + CC_{membrane} + CC_{equipment} + CC_{installation} \quad (3.35)$$

$$An_{Op,PV} = An_{replacment,PV} + An_{labor,PV} \quad (3.36)$$

$$An_{Op,Gen} = An_{fuel,Gen} + An_{replacment,G} + An_{Maintanance,G} \quad (3.37)$$

$$An_{Op,RO} = An_{replacment,RO} + An_{labor,RO} + An_{chem,RO} \quad (3.38)$$

The abbreviations (*chem*) for chemicals.

$$An_{fuel,Gen} = 365 \tau CC_{fuel} V_{fuel} \left[\frac{1 - (1+j)^n (1+i)^{-n}}{i-j} \right] \frac{i(1+i)^n}{(1+i)^n - 1} \quad (3.39)$$

Where,

τ	is the availability of RO plant (%).
C_{fuel}	is fuel cost in first year ($\frac{\$}{L}$).
V_{fuel}	is the fuel volume used per day ($\frac{L}{day}$).
j	is the escalation rate for fuel cost (%).

3.3. Validation of the model:

In this study, the introduced model with two software are used to analysis the hybrid diesel-PV powered RO system. Reverse Osmosis System Analysis software (ROSA) is used to simulate the RO system. Hybrid Optimization of Multiple Energy Resources software (HOMER) is used to simulate the power system. Equations and model are used to design the ERD, special RO configurations and to analyze the systems economics.

In this section, the work done by Bilton et al. [15] for brackish water RO desalination is used to validate the presented model. Table 5 lists the main input data for the system. The technical and economical results with the percentage error are listed in Table 6 and Table 7.

Table 5. Input Validation Data

Location	Pump Efficiency (%)	Permeate Flow Rate ($\frac{m^3}{h}$)	Water Density ($\frac{kg}{m^3}$)	Well Depth (m)	Pump Power (kW)
USA	70	1	997	120	0.465
Jordan	70	1	997	100	0.388
Australia	70	1	997	15	0.058
Tunisia	70	1	997	20	0.077

Table 6. Validation Power Results

Location	Model Power Consumption (kW)	Reference Power Consumption (kW)	Percentage Error (%)
USA	20.37	20.8	2.1
Jordan	19.28	19.9	3.1
Australia	18.69	18.4	1.6
Tunisia	16.59	16	3.7

Table 7. Validation Economic Results

Location		Model LCOW ($\frac{\$}{m^3}$)	Reference LCOW ($\frac{\$}{m^3}$)	Percentage Error (%)
USA	PV	2.36	2.41	2.1
	Gen	3.81	3.85	1
Jordan	PV	2.45	2.36	3.8
	Gen	3.7	3.75	1.3
Australia	PV	2.2	2.17	1.4
	Gen	3.6	3.48	3.4
Tunisia	PV	2.35	2.28	3.1
	Gen	3.19	3.34	4.5

Chapter 4:

Performance and Cost Analyses for Ummluj Well

4.1. Introduction:

In this chapter, performance and cost analyses are conducted for hybrid diesel-PV powered RO system to desalinate a well water in a village near Ummluj city. There are two main sides in this study: Energy production side and desalination side. In the energy side, the study starts with using diesel as the only power source. Then, the PV penetration is increased gradually up to 100%. In addition, the study investigates the effect of changing the diesel price. Regarding RO side, two modes are studied. First, batch RO system that operates 5 hours per day. Second, continuous RO system that operates 24 hours per day. In each mode, the benefit of using the pressure exchanger device as an energy recovery device is analyzed. Furthermore, the study compares between one and two stages RO systems. Figure9 summarizes RO options in this study. Also, the effect of adding second storage tank for household purpose is studied .In the next chapter, the study compares results of five different locations in KSA including this location.

First step to study the system is to collect the environmental resources for the project location, water quality and the needed permeate water flow rate.

Second step is to design the RO system and simulate it in ROSA software. If the system has more than one water storage tank, the new permeate flow rate must be calculated before the RO design. The third step is to utilize the information gathered so far to design the power system and simulate it using HOMER software to find the optimum system. If the PX is used in the system, the effect of the ERD must be calculated. Final step is to study the economics of the whole system. Figure10 illustrates the flow chart for this study.

In this chapter, detailed calculations are described for one case under the batch mode. This case is the one stage system with pressure exchanger and two tanks, which cover all important design steps. In addition, the results for other cases are shown.

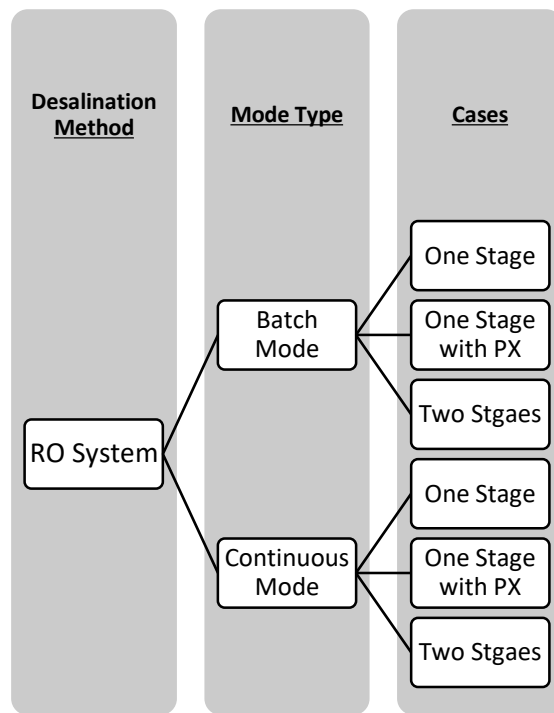


Figure9 . RO Modes and Cases in This Study

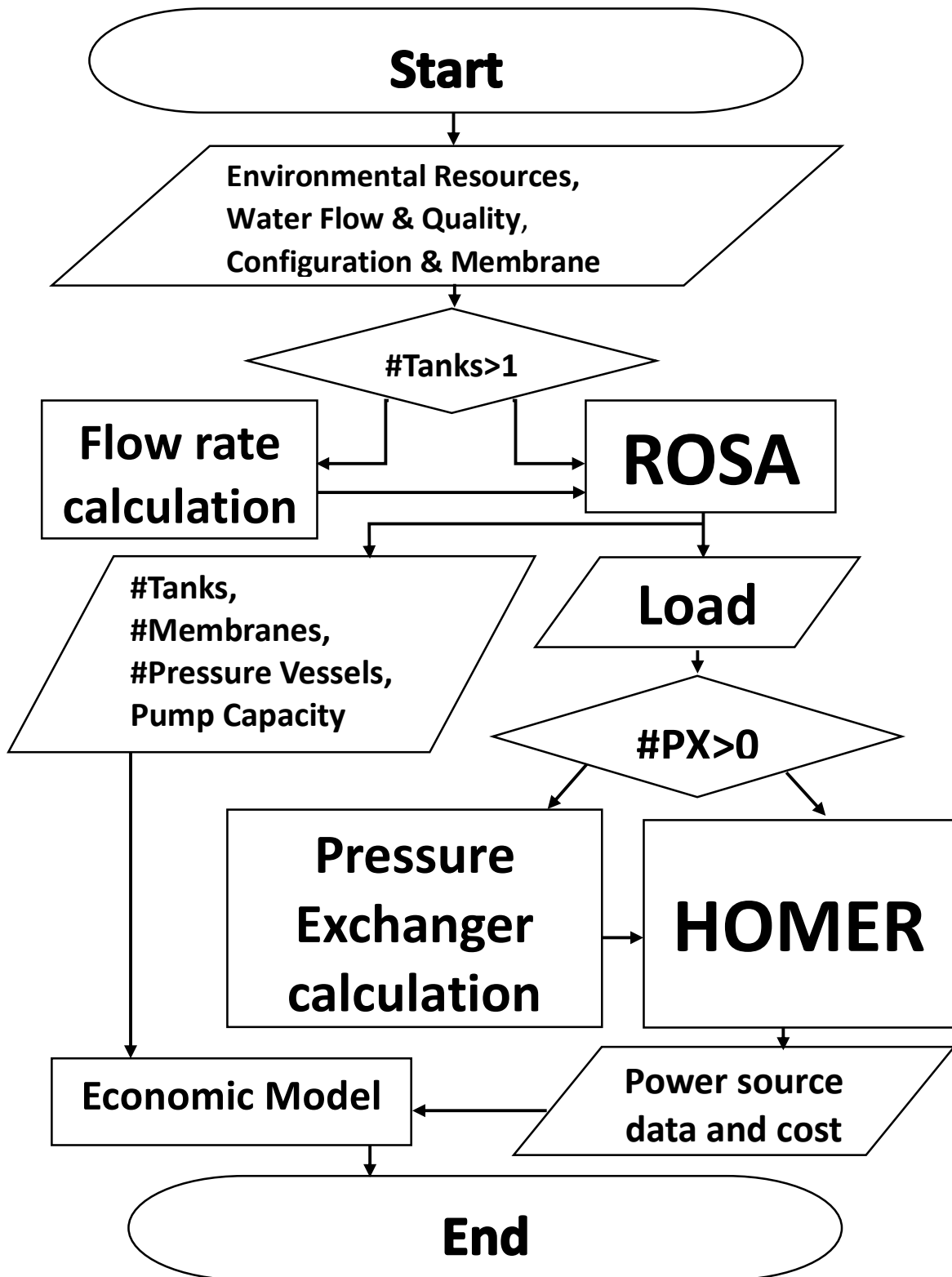


Figure10 . Study Flow Chart

4.2. Data Collection:

In this study, our target is to desalinate a well water with 6000 *ppm* salinity for two purposes: drinking and other household applications such as washing. According to El-Dessouky and Ettouney, the good salinity of drinking water should be 150 *ppm* or less where the municipal application should be 2000 *ppm* or less [4]. The proposed system will be located in a village near Ummluj city supplying water to a population of 1000 person. Table 8 summarizes the important information.

Table 8. Well and Production Information

Number of Beneficiaries		1000 Persons
Feed Source		Well Water
Feed Quality		6000 <i>ppm</i>
Well Depth		50 <i>m</i>
Average consumption per capita	Municipal	200 $\frac{\text{Liter}}{\text{day}}$
	Drinking	2 $\frac{\text{Liter}}{\text{day}}$
Product Quality	Municipal	1000 ppm
	Drinking	150 ppm
Daily Product Flow	Municipal	200 $\frac{\text{m}^3}{\text{day}}$
	Drinking	2 $\frac{\text{m}^3}{\text{day}}$

The village is located in the west of Saudi Arabia. Table 9 lists the Global Horizontal Irradiance (GHI) data, wind speed data and the temperature data According to NASA Surface Meteorology and Solar Energy Database [36]. From the

daily radiation data, the yearly average value is $5.9 \frac{kWh}{m^2}$ per day, which means that at standard test condition (STC) the solar panel produces its nominal productivity for 5.9 hours. However, this number reduces to approximately 5 hours when the temperature effect is accounted. For this reason, the batch mode in this study is assumed to operate 5 hours per day.

Table 9. Environmental Data [36]

Month	Clearness Index	Daily Radiation ($\frac{kWh}{m^2}$ per day)	Average Wind Speed $\frac{m}{s}$	Daily Temperature (°C)
January	0.631	4.240	5.220	16.670
February	0.651	5.100	5.080	17.820
March	0.653	6.030	5.260	21.040
April	0.651	6.780	5.020	25.760
May	0.646	7.140	4.700	29.900
June	0.693	7.780	4.750	32.390
July	0.670	7.440	4.430	32.500
August	0.655	6.940	4.350	33.090
September	0.651	6.250	4.450	32.350
October	0.635	5.220	4.520	28.370
November	0.626	4.350	4.530	22.960
December	0.616	3.910	4.890	18.540

4.3. RO System Design for First Case:

In this study, the water is assumed to be an incompressible water with 997

$\frac{kg}{m^3}$ density and 25°C temperature. The detailed chemical analysis for the water is

ignored. However, the RO design built based on the general total dissolve solution (TDS).

4.3.1. Membranes and Pressure Vessels Design:

The first step to design a reverse osmosis system is to select the membrane type and the average system flux. The membrane type selection depends on the feed salinity, fouling, product quality and system energy. According to DOW manual, the suitable membrane for our application is BW30-400 [5]. Table 10 lists the characteristics of BW30-400 membrane from DOW Company. The recommended membrane flux for wells source is between 27 and 34 $\frac{Liter}{m^2.h}$ [5]. Thus, the assumption of flux (f) in this study is 30 $\frac{Liter}{m^2.h}$.

Table 10. Membrane Characteristics

Name	Active Area	Pressure	Flow	Max. Recovery
BW30-400	37 m^2	15.5 bar	40 $\frac{m^3}{day}$	15 %

The number of membrane elements needs in this project could be calculated using the following formula:

$$N_E = \frac{Q_p}{f \cdot S_E} \quad (4.1)$$

Where,

Q_p is the hourly permeate flow rate for the system ($\frac{m^3}{h}$).

f is the flow flux ($\frac{m^3}{m^2 \cdot h}$).

S_E is the membrane active area (m^2).

In the case of batch mode and one tank, the hourly permeate flow rate should be $40.4 \frac{m^3}{h}$. However, if we add another water storage tank for household purposes with 1000 *ppm* salinity, the hourly permeate flow rate will be less because we can mix the RO production with the feed as describes in Figure11 . Thus, the hourly permeate flow rate becomes $34.3 \frac{m^3}{h}$ which is calculated using equations 3.11, 3.12 and 3.13 with trial and error method.

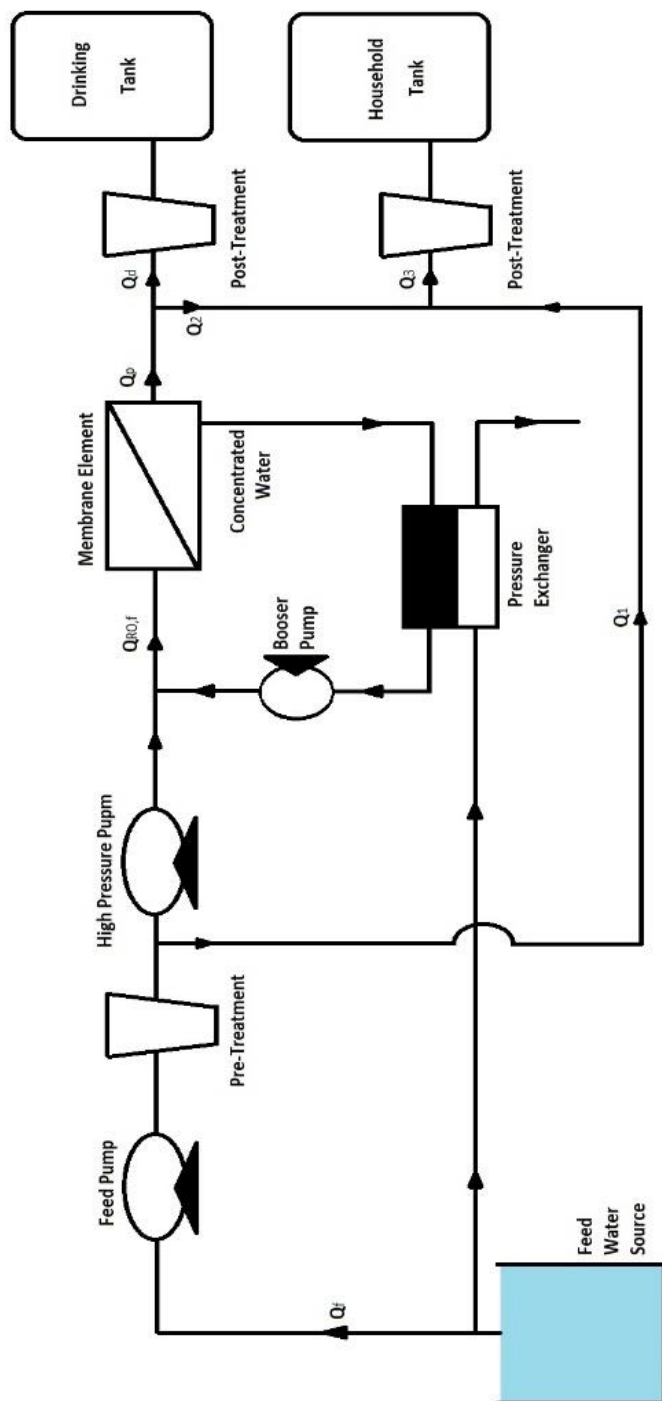


Figure11 . RO System with Two Tanks and PX

Now,

$$N_E = \frac{34.3}{0.03 \times 37} = 30.9 \approx 31 \text{ Elements.}$$

Next step is to calculate the number of pressure vessels (N_V). According to DOW manual, the pressure vessel should contain between 6 and 8 membranes [5].

$$N_V = \frac{N_E}{N_{EpV}} \quad (4.2)$$

Where,

N_{EpV} is the number of elements per vessel.

Now,

$$N_V = \frac{31}{6} = 5.167 \approx 5 \text{ Pressure Vessels.}$$

Thus, the RO system contains five pressure vessels with six membranes in each one. The flow flux becomes $31 \frac{\text{Liter}}{\text{m}^2 \cdot \text{h}}$, which is within the recommended range.

4.3.2. ROSA Results:

The system is a single stage type with 50% recovery ratio (RR) as recommended for one stage type [5]. To analyze the system and find the optimum system, ROSA software is used. The results show that the feed flow from the well to the system is $68.6 \frac{m^3}{h}$ with 6000 *ppm* salinity at 21.15 *bar*. Fifty percent of the feed produces as permeate flow with 67.15 *ppm*, while the rest is lost as brine with 11,933.73 *ppm* at 18.69 *bar*. The feed and the concentrated osmotic pressures are 4.74 and 9.34 *bar*, respectively. The results demonstrate in Figure 12 and Figure 13 .

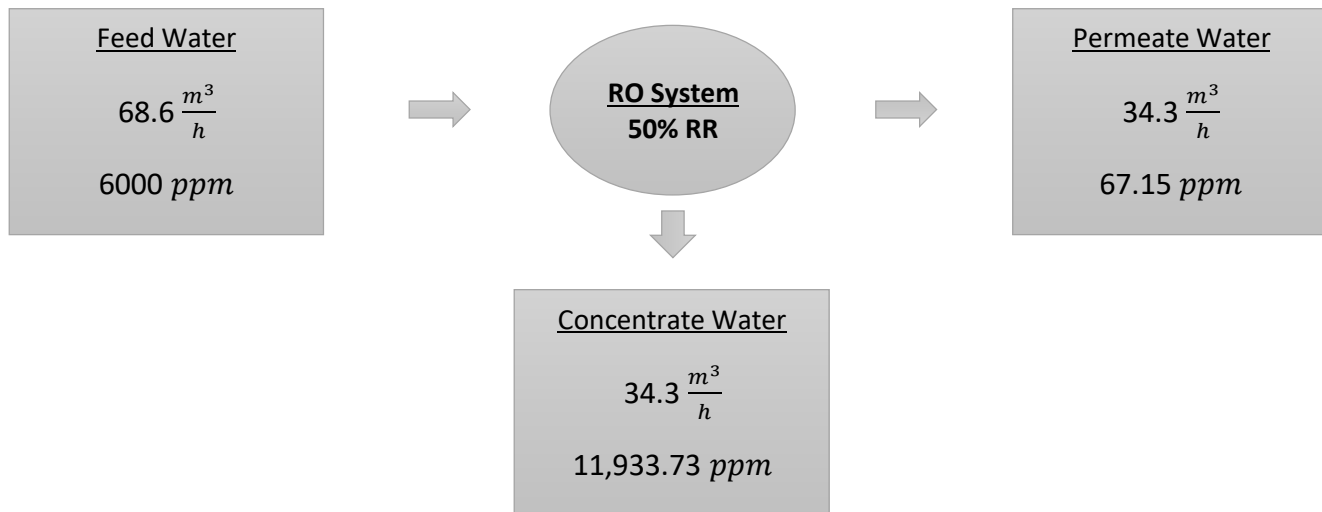


Figure12 . RO System Summary

Project Information:

Case-specific: plug flow, batch mode (5 hours), for two tanks and one stage system without PX

System Details

Feed Flow to Stage 1	68.60 m³/h	Pass 1 Permeate Flow	34.30 m³/h	Osmotic Pressure:	
Raw Water Flow to System	68.60 m³/h	Pass 1 Recovery	50.00 %	Feed	4.74 bar
Feed Pressure	21.15 bar	Feed Temperature	25.0 C	Concentrate	9.34 bar
Flow Factor	0.85	Feed TDS	6000.01 mg/l	Average	7.04 bar
Chem. Dose	None	Number of Elements	30	Average NDP	12.77 bar
Total Active Area	1114.80 M²	Average Pass 1 Flux	30.77 l/mh	Power	50.40 kW
Water Classification: Well Water SDI < 3				Specific Energy	1.47 kWh/m³

Stage	Element	#PV	#Ele	Feed Flow (m³/h)	Feed Press (bar)	Recirc Flow (m³/h)	Conc Flow (m³/h)	Conc Press (bar)	Perm Flow (m³/h)	Avg Flux (l/mh)	Perm Press (bar)	Boost Press (bar)	Perm TDS (mg/l)
1	BW30-400	5	6	68.60	20.81	0.00	34.30	18.69	34.30	30.77	0.00	0.00	67.15

Pass Streams (mg/l as Ion)					
Name	Feed	Adjusted Feed	Concentrate	Permeate	
			Stage 1	Stage 1	Total
NH4+ + NH3	0.00	0.00	0.00	0.00	0.00
K	0.00	0.00	0.00	0.00	0.00
Na	2360.25	2360.25	4694.42	26.41	26.41
Mg	0.00	0.00	0.00	0.00	0.00
Ca	0.00	0.00	0.00	0.00	0.00
Sr	0.00	0.00	0.00	0.00	0.00
Ba	0.00	0.00	0.00	0.00	0.00
CO3	0.00	0.00	0.00	0.00	0.00
HCO3	0.00	0.00	0.00	0.00	0.00
NO3	0.00	0.00	0.00	0.00	0.00
Cl	3639.76	3639.76	7239.29	40.73	40.73
F	0.00	0.00	0.00	0.00	0.00
SO4	0.00	0.00	0.00	0.00	0.00
SiO2	0.00	0.00	0.00	0.00	0.00
Boron	0.00	0.00	0.00	0.00	0.00
CO2	0.00	0.00	0.00	0.00	0.00
TDS	6000.01	6000.01	11933.73	67.15	67.15
pH	N/A	N/A	N/A	N/A	N/A

Figure 13. ROSA Results

The power required to operate the high-pressure pump is 50.4 kW , when the pump efficiency is 80%. In the industry, the power required for pretreatment and posttreatment processes is, approximately, 15% of the high-pressure pump capacity. Therefore, the high-pressure pump consumption becomes 57.96 kW . The feed water pump consumption must be added to find the total required power. The feed pump consumes 5.49 kW according to equation 7, where the well depth is 50 m and the pump efficiency is 85%. Now, the total power required to operate the system is 63.45 kW , which is calculated using equation 9. Thus, the specific energy for the system becomes $1.85 \frac{\text{kWh}}{\text{m}^3}$, which is calculated using equation 10.

Table 11. Pumps Power Consumptions

Load Type	Consumption (kW)
High-Pressure Pump	50.4
Pre-Treatment	7.56
Feed Water Pump	5.49
Total	63.45

4.4. Energy Optimization for First Case:

To find the optimum energy system from economical point of view, HOMER software is used. In order to obtain accurate results from HOMER, detailed information about the energy system should be supplied to the software.

4.4.1. ERD Calculation:

From the previous results, the power required to operate the RO system is 63.45 kW . Note that $34.3 \frac{\text{m}^3}{\text{h}}$ of water at 18.69 bar is lost as brine. To recover this energy, pressure exchanger device (PX) is used. According to Energy Recovery Company, the suitable pressure exchanger for this case is PX-180 with 96.7% efficiency [37]. From equation 6, the output power of the pressure exchanger is 17.22 kW . Thus, the RO system power consumption after using PX is 46.23 kW .

4.4.2. Load Information:

The load in this study is the RO system consumption, which is 46.23 kW in the chosen case. The RO system works 5 hours per day. Thus, the daily energy consumption is 231.15 kWh . The type of load is an electric load. Deferrable electric load function is used to define our system since the system must works

five continuous hours regardless of the exact operation time. To avoid the problem of power outage due to inconsistency in solar irradiance, water tanks are treated as storage for three days product. Figure 14 is a screen shot from load information in HOMER.



Figure 14. HOMER Load Information

4.4.3. Energy Source Information and Emission:

In this study, three energy sources are used: Diesel Generator, PV Panels and Electric Batteries. The generator produces AC electrical power, while PV and batteries produce DC electrical power. Thus, an inverter must be added to convert DC to AC and vice versa. The fuel type for the generator is Diesel. Table 12 lists the fuel properties.

The Photo-Voltaic Panels is a flat plate module with 17% efficiency, -0.45% /°C Temperature Coefficient and 25 years lifetime. Batteries are lead acid type with 5 years lifetime. Energy information and emission for different solar penetration are listed in Table 13. The emission produces during PV manufacturing is ignored.

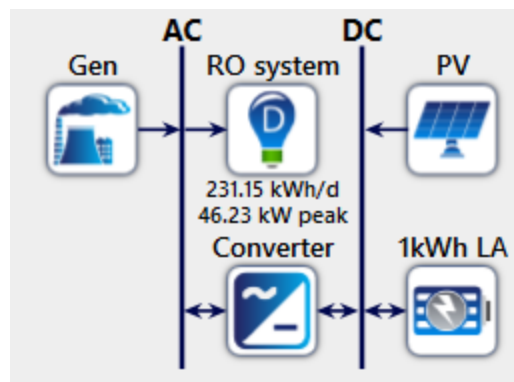


Figure 15. System Schematic

Table 12. Fuel Properties

Fuel Type	Lower Heating Value (MJ/kg)	Density (kg/m ³)	Carbon Content (%)	Sulfur Content (%)
Diesel	43.2	820	88	0.4

Table 13. Energy and Emission Information

Renewable Fraction	PV (kW)	Gen (kW)	Battery (kWh)	Converter (kW)	Excess Electricity (kWh/yr)	Percentage of Excess Electricity	CO ₂ Emission (kg/yr)	CO ₂ Saving (kg/yr)
100.0%	141	0	0	49	146,893.00	62.4%	0.0	63,380.0
90.8%	99.3	47	1	46.9	85,816.00	49.5%	6,012.0	57,368.0
81.0%	91.6	47	1	46.9	81,484.00	48.3%	12,472.0	50,908.0
72.6%	87	47	4	46.6	81,267.00	48.3%	17,927.0	45,453.0
62.7%	80.9	47	17	47.9	79,778.00	48.0%	24,290.0	39,090.0
51.6%	76.3	47	5	51.6	81,869.00	48.8%	31,789.0	31,591.0
42.7%	72	47	13	48	82,473.00	49.1%	37,491.0	25,889.0
32.5%	66.9	47	17	48.8	83,026.00	49.4%	44,293.0	19,087.0
21.5%	54	47	21	49.6	71,240.00	45.7%	51,574.0	11,806.0
13.2%	38	47	1	19.8	51,759.00	38.1%	51,221.0	12,159.0
0%	0	47	0	0	0	0%	63,380.0	0

4.5. Economic Study for the First Case:

In this study, net present value (NPV) technique is used to analyze all cash flows with 5% discount rate. Note that the techniques used in all model and software are similar. For comparison purpose, annualized net present value is derived. The aim is to find the best techno economic case, which has high

renewable penetration with low levelized cost of water (LCOW). Details cost investigations are analyzed for both sides: RO and Energy. The expected lifetime for this project is 25 years. All costs in this study are based on real quotations from local companies.

4.5.1. RO Economics:

For the chosen case, the system capital cost is \$162,565.4, which includes the price of labor recruitment, high-pressure pump, feed water pump, membranes, pressure vessels, pretreatment, post treatment, all other RO components and construction work. Table 14 gives the cost data. The feed water pump is replaced every 10 years, while the high-pressure pump is replaced every 15 years. The cash flow chart for RO system illustrates in Figure16 . Figure 17represents the equivalent annualized cost. The net present value for the system is equal to \$403,911.8.

Table 14. RO System Cost Data

Cost Type	Price (\$)
System Capital Cost	162,565.4
PX Capital Cost	72,000
System O&M (include membrane replacement)	4,500
High-Pressure Pump Replacement	23,695
Feed Water Pump Replacement	2,600
Labor Salary per year	6,000
PX O&M	500

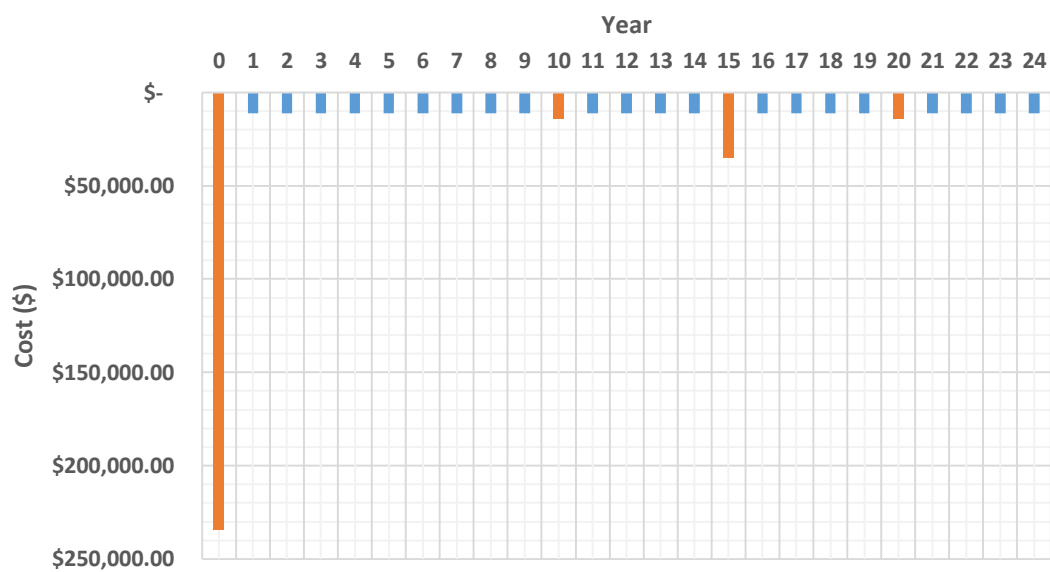


Figure16 . RO Cash Flow Chart

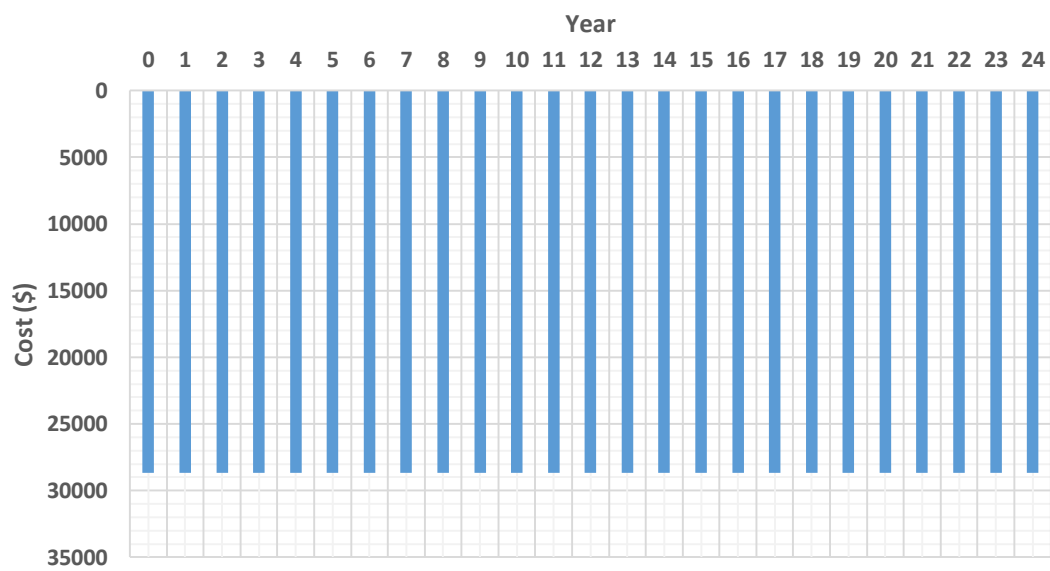


Figure17 . RO Annualized Cash Flow Chart

4.5.2. Energy Sources Economics:

In the energy side, the cost of three main components are accounted. First, diesel generator cost, which includes the capital cost, operation and maintenance cost, fuel cost and fuel transportation cost. Table 15 lists the cost data, while Figure 18 illustrates the relation between fuel consumption and output power. The fuel transportation cost is \$325 per year for one fill of fuel storage tank per month while the needed monthly number of refilling times depend on the penetration percentage of PV. If the PV penetration is less than 20%, the fuel tank has to be refilled 4 times per month. However, the fuel tank has to be refilled 3 times per month if the PV percentage is between 20% and 50%. If the percentage is between 50% and 80%, it needs to be refilled twice a month only. But, if the PV sharing more than 80%, the fuel tank needs to be refilled only once a month. Second, the cost of PV system, which include capital and operation cost for all components excluding the batteries. Figure 19 demonstrates the cost slope for PV system because the PV cost depend on the size of the system, starting from \$2,500 for 1 kW if the size is less than 10 kW down to \$1,500 for 1 kW if the size is 100 kW and bigger. If the size is between 10 kW and 100 kW, the price for 1 kW becomes \$2,000. Third, the batteries cost, which include the capital, O&M and replacement costs. All important information are listed in Table 16.

Table 15. Generator Cost Data

Size (kW)	Capital Cost (\$)	Annualized Capital Cost (\$/yr)	Lifetime (Hours)	Fuel Price (\$)	Fuel Transportation (\$/year/time)
47	23,500	1,667.38	15,000	0.13	325

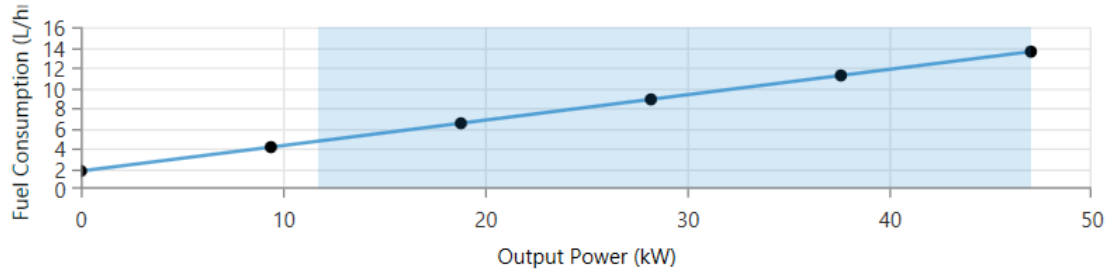


Figure 18. Fuel Consumption and Output Power Relation

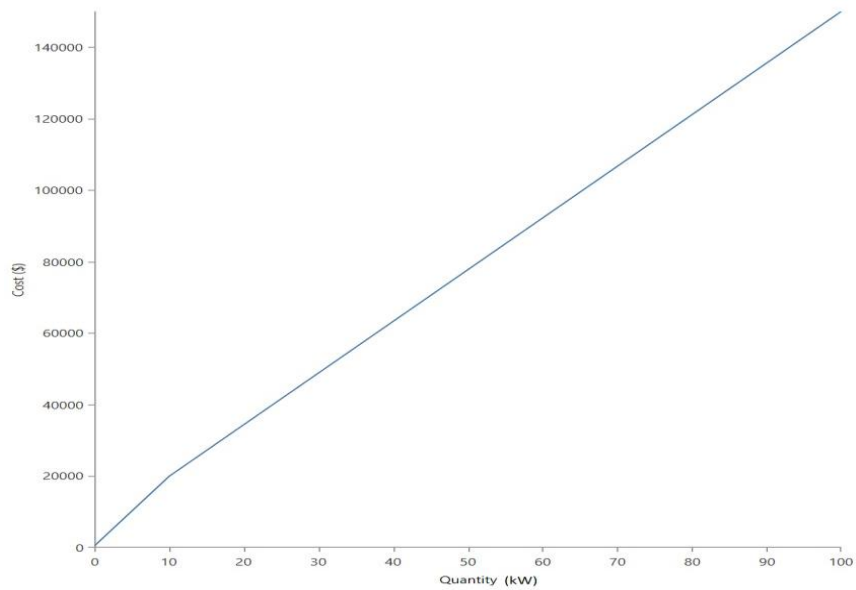


Figure 19. PV Cost Curve

Table 16. Battery Cost Data

Battery Type	Capital Cost (\$)	Replacement Cost (\$)	O&M (\$/yr)	Lifetime (years)
1 kWh lead acid batteries	300	300	10	5

4.5.3. Results for the First Case:

Depending on the previous analysis, LCOW and LCOE are calculated for different PV penetration percentages using equations 26 and 30. Results are listed in Table 17 and Figure 20. It is clear from the graph that the lowest water price happens when using 100% diesel generator at \$0.13 per liter of fuel. However, the best PV penetration from cost point of view is 85%. The slope of the cost function is positive up to its peak at 30% PV sharing, which means increasing in the cost because of the foundation of PV system. After 30%, the trend is declined until 85%. In this range, the benefit of adding PV system appears. The negative slope is due to reduction in fuel consumption and fuel transportation. However, the cost curve rises again due to the large increasing in the PV size to meet the load in days that have lowest solar irradiance.

Table 17. Detailed Cost Results for Batch Mode, Two Tanks with PX

PV Penetration	$An_{CC,PV}$	$An_{Op,PV}$	$An_{CC,G}$	$An_{Op,G}$	$An_{CC,RO}$	$An_{Op,RO}$	An_{total}	LCOW (\$/m ³)	LCOE (\$/kWh)	Energy Cost Percentage	RO Cost Percentage
100.00%	\$14,854.56	\$645.66	\$0.00	\$0.00	\$16,642.99	\$12,016	\$44,158.76	0.898388	0.18	64.90%	35.10%
90.80%	\$10,594.54	\$657.25	\$1,667.38	\$586.25	\$16,642.99	\$12,016	\$42,163.96	0.857805	0.16	67.97%	32.03%
81.00%	\$9,798.28	\$648.61	\$1,667.38	\$1,422.35	\$16,642.99	\$12,016	\$42,195.16	0.858439	0.16	67.92%	32.08%
72.60%	\$9,395.68	\$817.56	\$1,667.38	\$2,441.05	\$16,642.99	\$12,016	\$42,980.21	0.874411	0.17	66.68%	33.32%
62.70%	\$9,049.01	\$1,564.91	\$1,667.38	\$3,365.86	\$16,642.99	\$12,016	\$44,305.70	0.901377	0.19	64.68%	35.32%
51.60%	\$8,321.78	\$863.68	\$1,667.38	\$4,620.73	\$16,642.99	\$12,016	\$44,132.11	0.897846	0.18	64.94%	35.06%
42.70%	\$8,048.90	\$1,322.88	\$1,667.38	\$5,746.92	\$16,642.99	\$12,016	\$45,444.62	0.924548	0.20	63.06%	36.94%
32.50%	\$7,616.40	\$1,549.38	\$1,667.38	\$6,834.62	\$16,642.99	\$12,016	\$46,326.32	0.942486	0.21	61.86%	38.14%
21.50%	\$6,379.32	\$1,767.07	\$1,667.38	\$7,977.54	\$16,642.99	\$12,016	\$46,449.85	0.944999	0.21	61.70%	38.30%
13.20%	\$4,308.37	\$589.09	\$1,667.38	\$8,583.48	\$16,642.99	\$12,016	\$43,806.86	0.891229	0.18	65.42%	34.58%
0.00%	\$0.00	\$0.00	\$1,667.38	\$8,866.87	\$16,642.99	\$12,016	\$39,192.79	0.797358	0.12	73.12%	26.88%

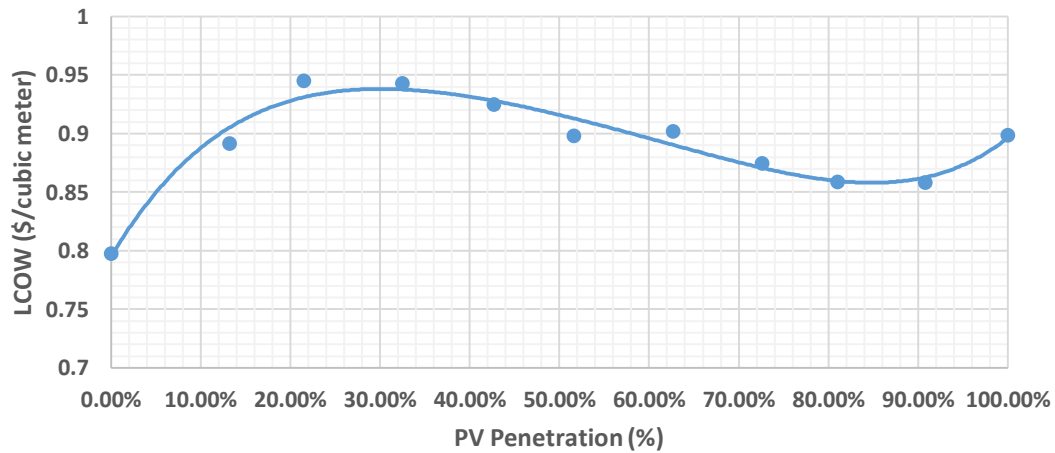


Figure 20. LCOW Curve for Batch Mode, Two Tanks with PX

4.6. Results for other cases:

In this section, results of all cases are analyzed and compared. The goal is to find the optimum case for our application. Similar design steps explained in the previous sections are followed.

4.6.1. Benefit of adding second storage tank:

The results show that adding a second storage tank for household purposes with salinity of 1000 *ppm* decreases the cost by 11% approximately. This effect is due to the reduction on the needed permeate water flow. This reduction decreases the high-pressure pump size and consumption. Table 18 demonstrates the benefit of adding another tank for batch mode without PX cases.

Table 18. Benefit of using Second Storage Tank

PV Penetration (%)	One Tank LCOW (\$/m ³)	Two Tanks LCOW (\$/m ³)	Reduction Percentage
100	1.014	0.895	12%
90	0.938	0.835	11%
80	0.936	0.835	11%
70	0.955	0.850	11%
60	0.965	0.865	10%
50	0.984	0.878	11%
40	1.008	0.904	10%
30	1.023	0.917	10%
20	1.000	0.896	10%
10	0.933	0.838	10%
0	0.835	0.751	10%
Average			11%

4.6.2. Batch Mode Vs. Continuous Mode:

The batch mode trends behave as explained in section 4.5.3 for all cases while the continuous mode trends have three behaviors. In the first segment, which is from 0% PV penetration until 20%, the trend is a linear function with low positive slope. In this range, the average solar penetration does not exceed the consumption of 4.8 hours per day, where 10% penetration cover the consumption of 2.4 hours per day. These 4.8 hours does not exceed the daily solar window (from 9 AM to 3 PM), where the solar irradiance is relatively high. Second segment has a linear function with sharper positive slope, which cover the range from 20% to 40% where the PV penetration does not exceed the consumption of 9.6 hours per

day. Thus, adding some batteries and increasing the PV size slightly is enough. The third segment behaves as a second order polynomial function. In this segment, every 10% renewable penetration means two and half hours more of night operation. Thus, a huge rising in the electrical storage size is expected with increasing in the PV modules to feed those batteries. At the end, the slope start to be negative due to low fuel consumption and low transportation price until 100% solar system is reached. Figure21 illustrates the relation between LCOW and PV penetration for all cases and modes. It is clear from the graph that if the PV sharing is less than 50%, the optimum mode is the continuous mode, while if the percentage of PV system is more than 50%, the optimum system is the batch mode.

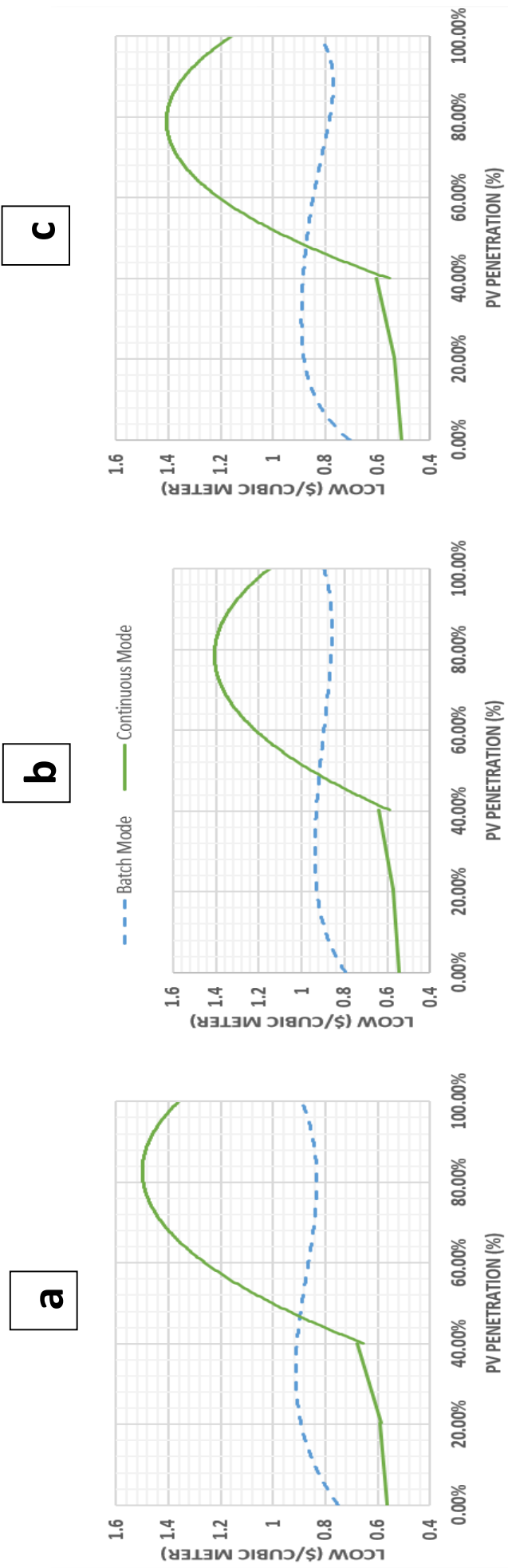


Figure21 . Batch Mode Vs. Continuous Mode (a:One Stage without PX, b:One Stage with PX ,c:Two Stages)

4.6.3. Cases Comparison:

The previous section demonstrates that the optimum RO mode for a case depends mainly on the PV penetration. However, what is the optimum case if the mode is fixed? For instance, is it better to design a one stage system with or without PX if the mode is batch? What about the two stages system? What if the mode is continuous? Answers of those questions are represented in Figure 22 and Figure 23. From the batch mode graphs, the optimum system from economic point of view is the two stages system. In addition, using pressure exchanger as energy recovery device in this mode is not feasible due to the high capital cost. This capital cost is higher than the cost of energy saved by PX device. However, LCOW if PX is used or not at 100% PV penetration are the same because the PV size in this case is very sensitive to the load size. On the other hand, the continuous mode graphs show that the two stages system is the optimum system. However, in this mode the PX is feasible to use in one stage system. The water recovery for all one stage systems is 50%, while it is 65% for two stages systems. The specific energy consumption (SEC) for one stage systems without PX is $1.84 \frac{kWh}{m^3}$ for batch mode while it is $1.9 \frac{kWh}{m^3}$ for continuous mode. For one stage with PX systems, they are $1.34 \frac{kWh}{m^3}$ and $1.4 \frac{kWh}{m^3}$ for batch and continuous modes, respectively. In the two stages systems, the SEC are $1.4 \frac{kWh}{m^3}$ and $1.48 \frac{kWh}{m^3}$. Figure 24 shows the water

recovery and SEC for all cases. From the previous results, using PX in the system leads to 26% reduction in the SEC. In addition, adding a second stage in the system reduces the SEC by 22%.

It is clear from the previous discussion that the optimum system for all modes in this area at \$0.13 per liter fuel price is the two stages system.

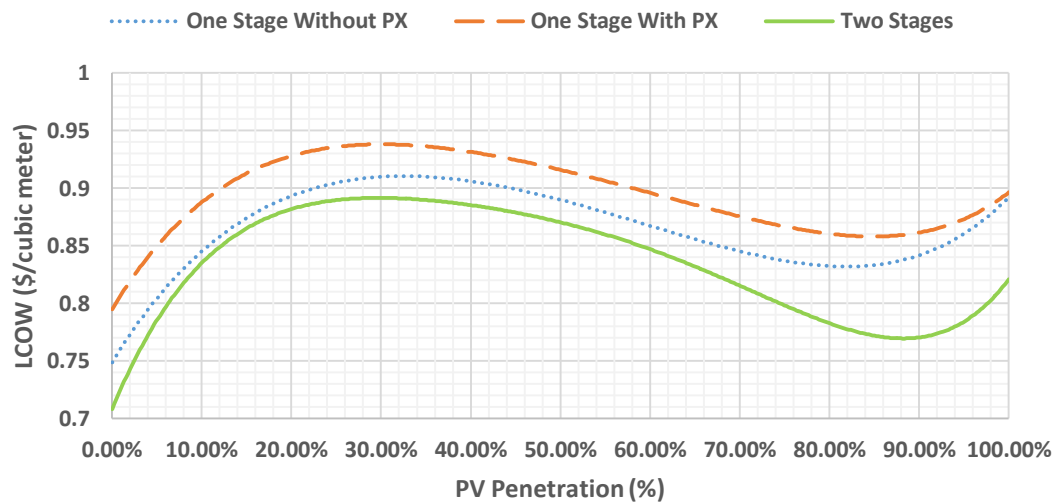


Figure 22. LCOE Vs. PV Penetration for Batch Mode Cases

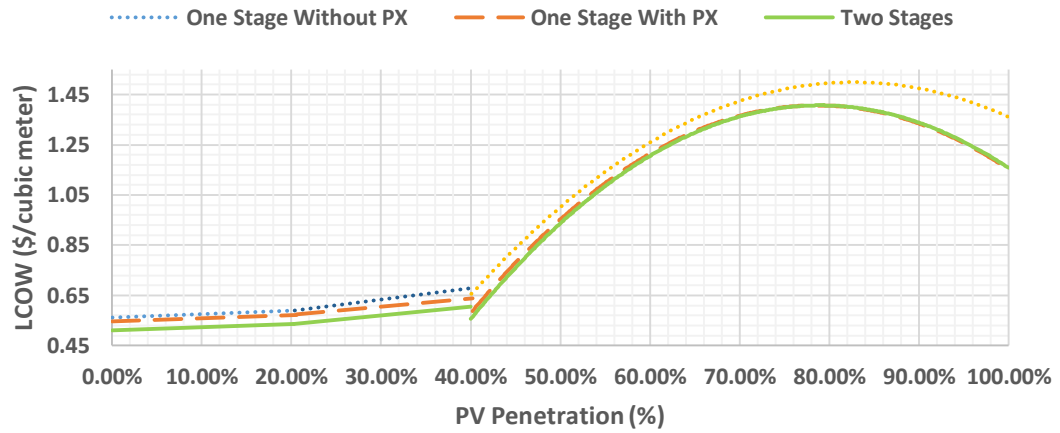


Figure 23. LCOW Vs. PV Penetration for Continuous Mode Cases

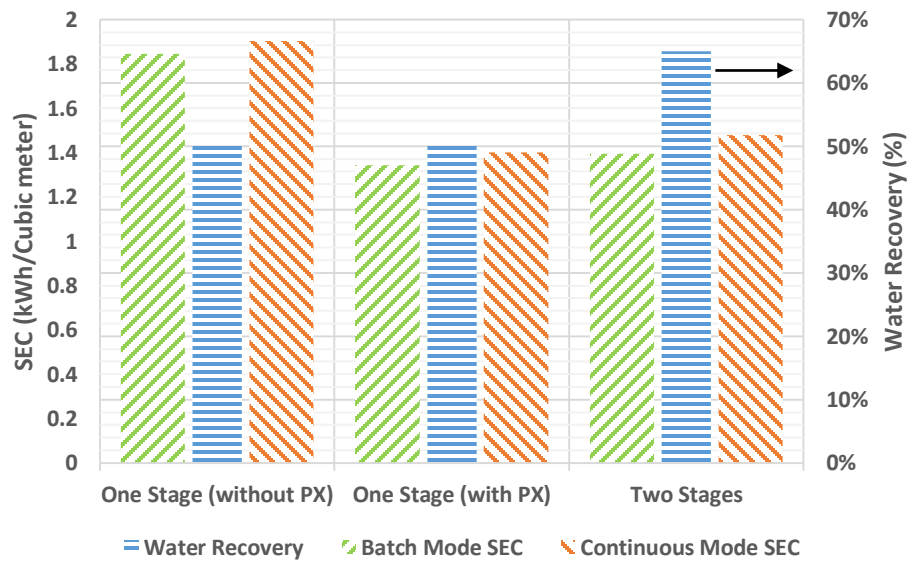


Figure24 . Water Recovery and SEC for Different Options

4.6.4. Effect of fuel price:

In this section, sensitivity analysis is performed to study the effect of fuel price on the results. At \$0.13 fuel price, the lowest LCOW in all cases is at 0% PV penetration. However, the results will change at different diesel price. The LCOW at 100% generator penetration for different fuel prices illustrates in Figure 25. The two stages system still has the lowest LCOW even if the fuel price is increased by 1,000%. Note that in the batch mode, the using of PX as ERD becomes feasible after the diesel price increases to \$0.4 per liter because at this rate, the cost of PX is less than the cost of fuel saved when using it. Figure 26 shows a comparison of different fuel prices for a two stages system in the batch mode. The lowest price happens at 85% PV penetration. At \$0.39 fuel price, the 100% PV penetration becomes more feasible than 100% generator penetration while in the continuous mode this happens at \$1.3 fuel price. In the continuous mode, adding PV up to 40% penetration becomes more feasible at \$0.65 and greater fuel price as Figure 27 demonstrates. In general, the lowest LCOW at 100% PV penetration is \$0.819 per cubic meter, which happens in the two stages batch mode. This cost does not affected by the fuel price. On the other hand, the lowest LCOW at 0% PV penetration happens in the two stages continuous mode. Thus, after \$0.68 diesel price the LCOW for 100% PV penetration in two stages batch mode becomes less than the LCOW for 0% PV penetration the two stages continuous mode. At \$0.65

fuel price and greater, which is four times today price, the optimum system becomes the two stages batch mode at 85% PV sharing.

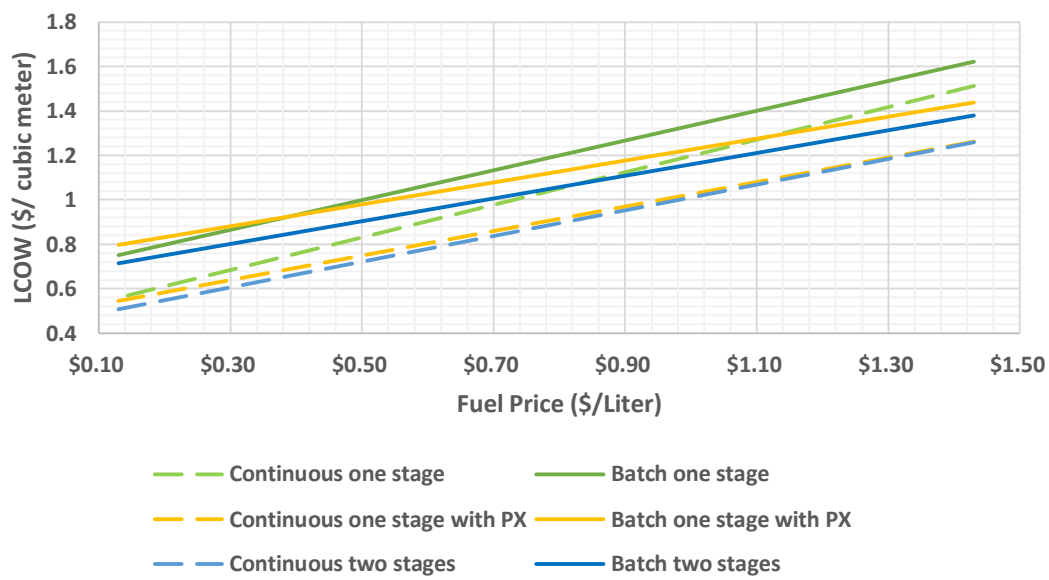


Figure 25. LCOW for Different Fuel Price at 100% Generator Penetration

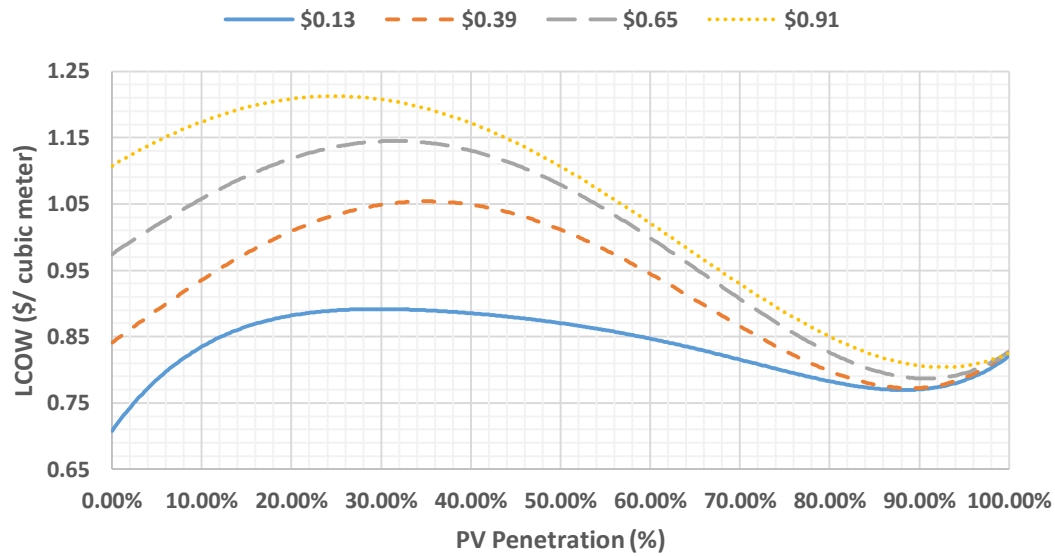


Figure 26. Different Fuel Prices Comparison for Batch Mode, Two Stages System

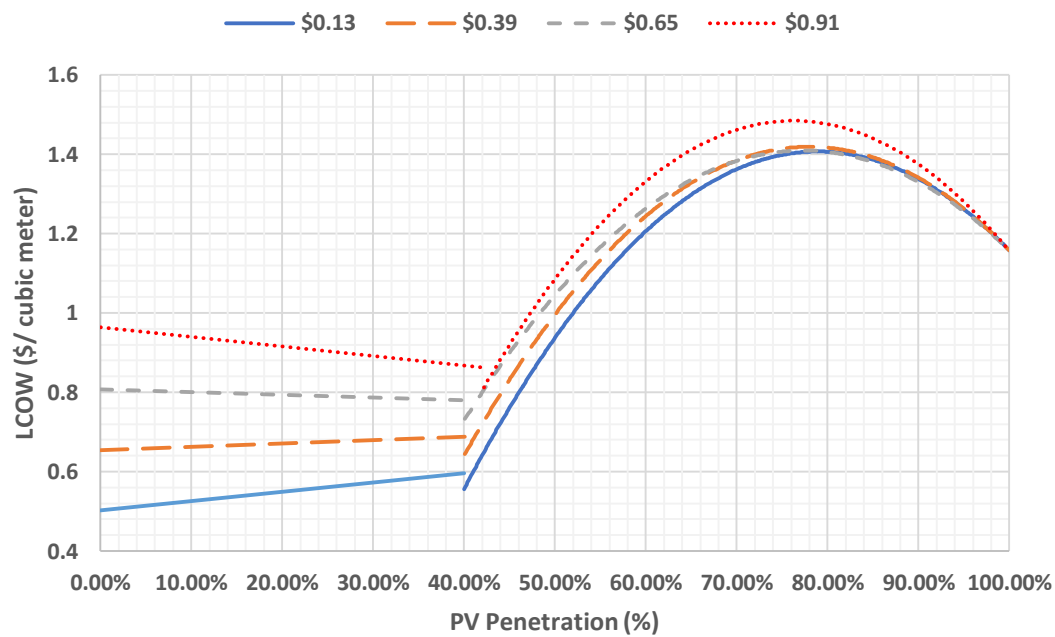


Figure 27. Different Fuel Prices Comparison for Continuous Mode, Two Stages System

Chapter 5:

Analyses of Five Different Locations in KSA

5.1. Introduction:

In the previous chapter, a complete analysis is performed for a brackish water well in a village near Ummluj city. Results show that the optimum RO system is the two stages option in either modes with two storage tanks. Thus, only this option is analyzed in this chapter.

In this chapter, a comparison is conducted to study the effect of system location on the results. Five different wells are compared, including Ummluj well. Each well has a salinity of 6000 *ppm*, but with different depths. The target for all locations is fixed, which is serving 1000 persons for drinking and household purposes.

First well is located in a village near Ummluj city in the west of Saudi and it has 50 *m* depth. Second well is located in a village near Buraydah city in the center of Saudi and it has 200 *m* depth. Third well is located in Haddar village near the south of KSA and it has 150 *m* depth. Fourth well is located in a village near Qaryat Al-Ulya city in the east of Saudi and it has 100 *m* depth. Fifth well is located in

Suhmah village in the eastern south of Saudi and it has 30 *m* depth. Figure28 illustrates locations and depths of the five wells.

In this study, the location has effects on three main parameters. First, the environmental resources such as solar irradiance, wind speed and temperature. Second, the fuel transportation cost. Third, the depth of the well.

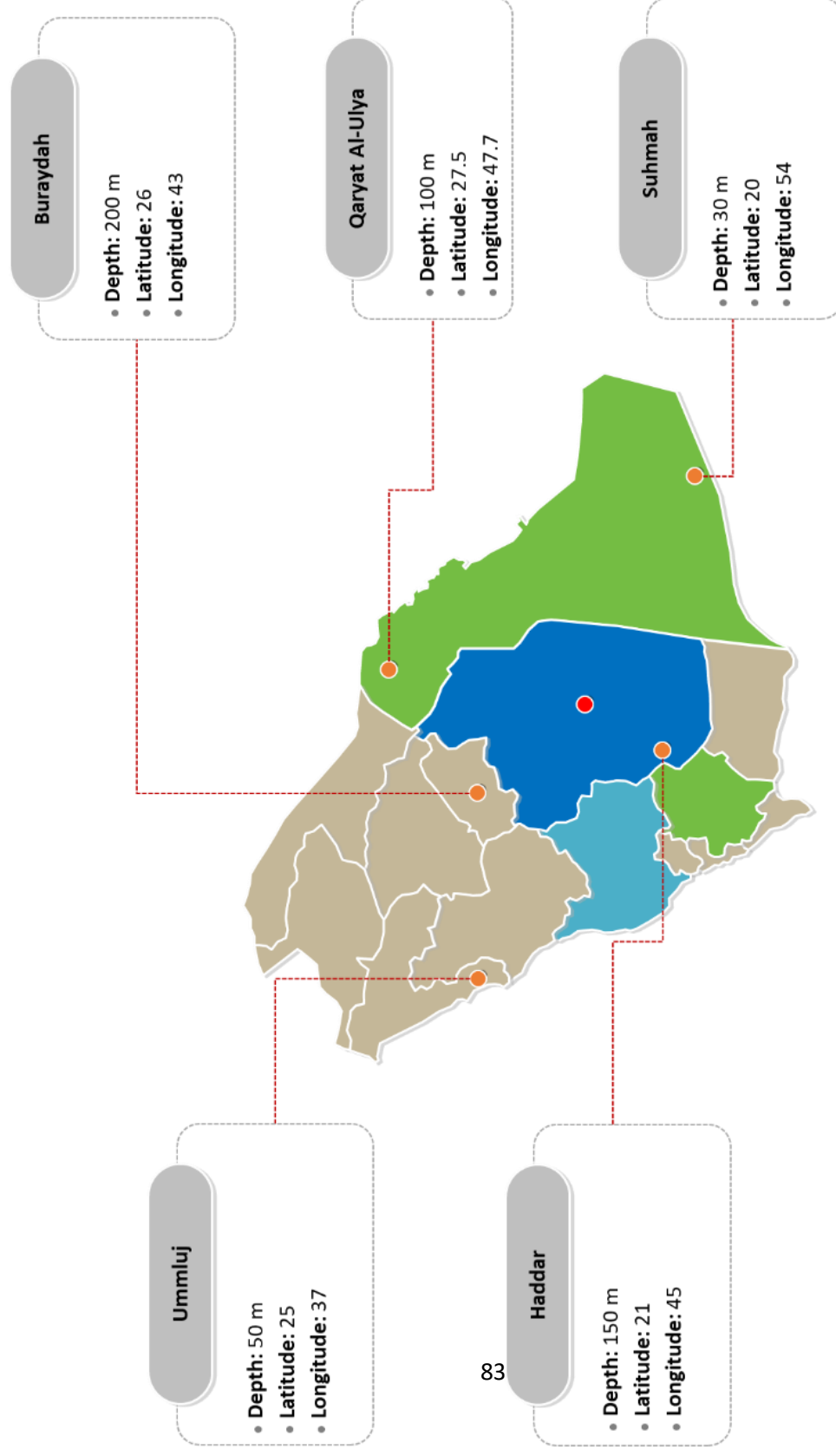


Figure28 . Locations of Five Wells

5.2. Locations Data:

As described in the previous section, the goal of each system is to desalinate brackish water with 6000 *ppm* salinity in different locations. Table 19 lists the Global Horizontal Irradiance (GHI) data, the wind speed data and the temperature data for the five locations according to NASA Surface Meteorology and Solar Energy Database [36].

Suhmah and Haddar are receiving the highest daily solar irradiance in comparison with others. In addition, Haddar has the highest average wind speed during the year. Furthermore, Buraydah has the lowest average daily temperature around the year. In general, Haddar has the best environmental conditions for PV applications.

5.3. Energy Consumption for each system:

Analyses in this chapter are focused in the two stages option with two water tanks. The only parameter that changes with location in the RO design is the size of feed water pump. This change is due to the variation in the well depth. Table 20 lists the feed water pump consumptions and the SEC for different locations and modes.

Table19 . Environmental Data for Five Locations [36]

Month	Clearness Index					Daily Radiation ($\frac{kWh}{m^2}$ per day)					Average Wind Speed ($\frac{m}{s}$)					Daily Temperature ($^{\circ}C$)				
	Ummiuj	Buraydah	Haddar	Qaryat	Suhmah	Ummiuj	Buraydah	Haddar	Qaryat	Suhmah	Ummiuj	Buraydah	Haddar	Qaryat	Suhmah	Ummiuj	Buraydah	Haddar	Qaryat	Suhmah
January	0.631	0.564	0.604	0.541	0.646	4.24	3.67	4.34	3.39	4.83	5.22	5.09	5.5	4.25	4.77	16.67	11.99	16.46	13.17	20.77
February	0.651	0.598	0.623	0.585	0.639	5.1	4.58	5.13	4.36	5.41	5.08	5.44	5.84	4.64	5.2	17.82	14.42	19.11	15.31	22.92
March	0.653	0.58	0.63	0.574	0.633	6.03	5.29	5.98	5.15	6.1	5.26	5.49	5.58	4.92	4.9	21.04	18.74	22.94	19.8	26.68
April	0.651	0.591	0.618	0.581	0.656	6.78	6.13	6.48	5.99	6.9	5.02	5.22	4.76	4.22	4.75	25.76	24.47	27.42	26.25	30.95
May	0.646	0.617	0.664	0.641	0.688	7.14	6.83	7.28	7.11	7.51	4.7	5.04	4.64	4.94	5.32	29.9	30.19	32.31	32.25	35.14
June	0.693	0.702	0.697	0.705	0.645	7.78	7.93	7.73	8	7.08	4.75	5.32	5.39	5.67	6.08	32.39	33.17	34.46	35.33	36.71
July	0.67	0.688	0.667	0.694	0.61	7.44	7.67	7.33	7.76	6.66	4.43	5.36	5.79	5.44	6.64	32.5	34.63	35.69	36.95	36.99
August	0.655	0.664	0.646	0.691	0.613	6.94	7.03	6.86	7.29	6.5	4.35	5.12	5.48	5.22	5.86	33.09	34.97	34.99	36.67	36.1
September	0.651	0.653	0.667	0.681	0.654	6.25	6.21	6.53	6.4	6.47	4.45	4.7	5.68	4.58	5.35	32.35	32.74	32.55	33.37	34.71
October	0.635	0.629	0.685	0.647	0.683	5.22	5.07	5.87	5.1	6	4.52	4.86	5.36	4.08	4.34	28.37	27.55	27.43	28.27	30.63
November	0.626	0.542	0.648	0.56	0.674	4.35	3.66	4.8	3.65	5.17	4.53	5.38	5.35	4.33	4.16	22.96	20.07	22.42	21.2	26.24
December	0.616	0.538	0.608	0.493	0.639	3.91	3.3	4.16	2.9	4.56	4.89	5.11	5.36	4.25	4.79	18.54	14.22	18.22	15.42	22.58
Average	0.648	0.614	0.646	0.616	0.648	5.932	5.614	6.041	5.592	6.099	4.767	5.178	5.394	4.712	5.180	25.949	24.763	27.000	26.166	30.035

Table 20. Feed Pump Consumption and SEC for Different Locations

Location	Well Depth (m)	Mode	Feed Pump Consumption (kW)	SEC ($\frac{kWh}{m^3}$)
Buraydah	200	Batch	21.97	1.87
		Continuous	4.56	1.96
Haddar	150	Batch	16.48	1.72
		Continuous	3.42	1.80
Qaryat Al-Ulya	100	Batch	10.98	1.56
		Continuous	2.28	1.64
Ummluj	50	Batch	5.50	1.40
		Continuous	1.14	1.48
Suhmah	30	Batch	3.30	1.33
		Continuous	0.68	1.41

5.4. Results:

After analyzing all systems as described in chapter four, results can be discussed in four aspects. First, the effect of environmental resources on the LCOW. Second, LCOW and PV penetration relation after adding the effect of well depth and fuel transportation for each system. Third, the LCOE for each system at 100% PV penetration. Fourth, the feasibility of adding PV panels to the system for different fuel prices. In addition, the effect of second storage tank salinity on the systems is studied.

5.4.1. Effect of Environmental Resources on the Results:

The aim of this section is to investigate the effect of environmental resources on the results, with fixing other parameters such as well depth. The design of Ummluj system is copied for other locations with same well depth and fuel transportation cost. Table 21 demonstrates the effect of environmental resources on the LCOW and PV system size for 100% PV penetration. Results show that Haddar, Suhmah and Ummluj have the best resources. Qaryat Al-Ulya has the worst resources. Those results show that environmental resources have a significant effect on the project cost. For instance, applying the same system in Qaryat Al-Ulya instead of Haddar increases the total cost by \$500,000 during the project lifetime.

Table 21. Effect of Environmental Resources on the LCOW and PV System Size for 100% PV Penetration

Mode	Location	LCOW($\frac{\$}{m^3}$)	PV Size (kW)	Batteries Size (kWh)
Batch	Buraydah	0.983	224	0
	Haddar	0.789	132	0
	Qaryat Al-Ulya	1.0195	242	0
	Ummluj	0.819	146	0
	Suhmah	0.816	145	0
Continuous	Buraydah	1.373	244	356
	Haddar	1.167	146	357
	Qaryat Al-Ulya	1.429	265	363
	Ummluj	1.156	137	362
	Suhmah	1.161	122	354

5.4.2. LCOW for Different PV Penetration:

After adding the effects of well depth and fuel transportation for all systems, LCOW curves have similar behaviors in the batch and continuous modes, which are explained in section (4.6.2). Thus, for system with PV penetration less than 40%, continuous mode is more feasible than batch mode. However, batch mode becomes more feasible after 40% PV sharing. Figure29 and Figure30 show the LCOW curves with respect to PV penetration for different locations. Note that

Suhmah system has double fuel transportation price since it is far away from the diesel station. Thus, Suhmah has higher LCOW than Ummluj at 0% PV penetration although it has lower power consumption.

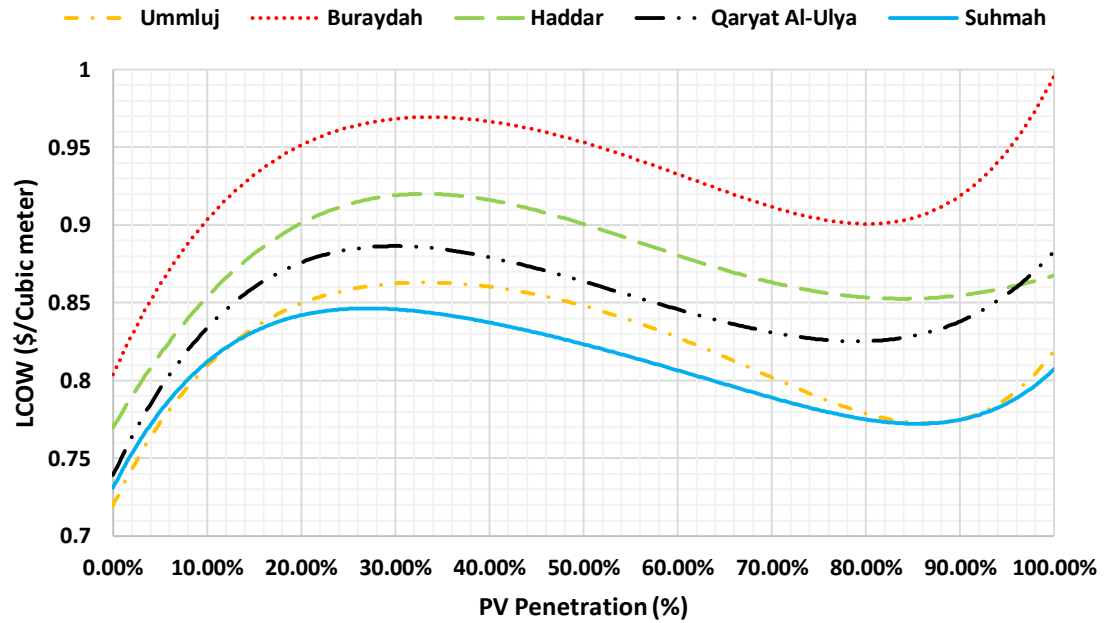


Figure29 . LCOW Vs. PV Penetration for Batch Mode Systems

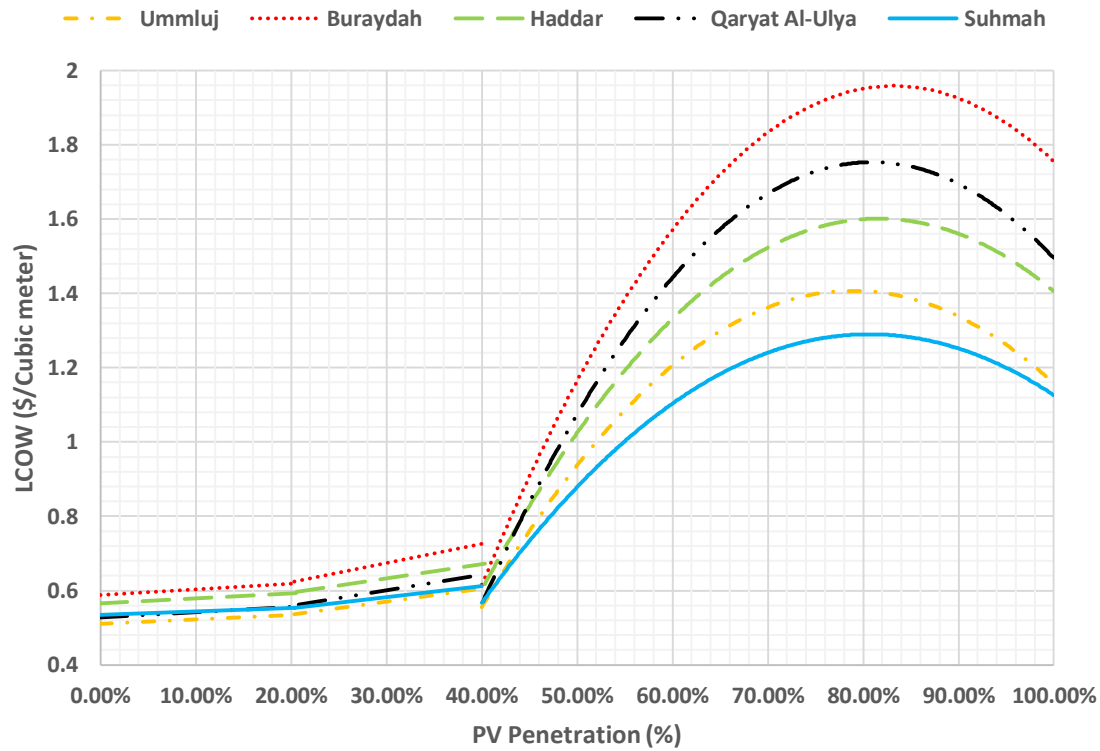


Figure30 . LCOE Vs. PV Penetration for Continuous Mode Systems

5.4.3. LCOE for Each System:

LCOE represents the cost of energy regardless of the RO cost. It indicates the feasibility of using PV in a location. Figure 31 shows the LCOE for different locations at 100% PV penetration. Haddar has the best value since it has good environmental resources and climate conditions for solar applications. Because

Buraydah and Qaryat Al-Ulya have relatively low solar irradiances, they have high LCOE.

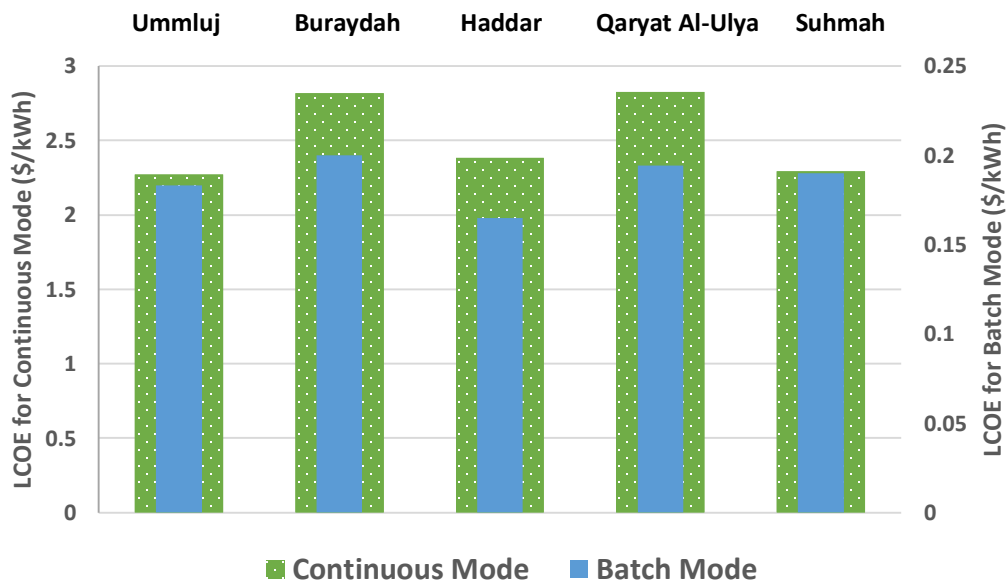


Figure 31. LCOE for Different Locations at 100% PV Penetration

5.4.4. Effect of Fuel Price:

In this section, sensitivity analysis is performed to study the effect of fuel price on the feasibility of adding PV to the power system. At today price (\$0.13 per liter), it is more feasible to operate the RO system with diesel generator only. However, this situation will change at different fuel price. Figure 32 illustrates the breakeven points for different locations, where adding PV to the system becomes

more feasible than 0% PV penetration. The figure presents the breakeven points at two different PV penetration percentage. First is 100% PV penetration, which present the system without diesel generator. The second PV penetration percentage is 85%, where the system has the lowest LCOW as describes in the previous results. This figure shows that Haddar has the lowest breakeven points. Those points are \$0.55 and \$0.57 for 85% PV penetration and 100%, respectively. Points for Suhmah are \$0.56 and \$0.63. For Ummluj, points are \$0.6 and 0.67. In Buraydah, points are \$0.55 and \$0.68. Points for Qaryat Al-Ulya are \$0.62 and \$0.72.

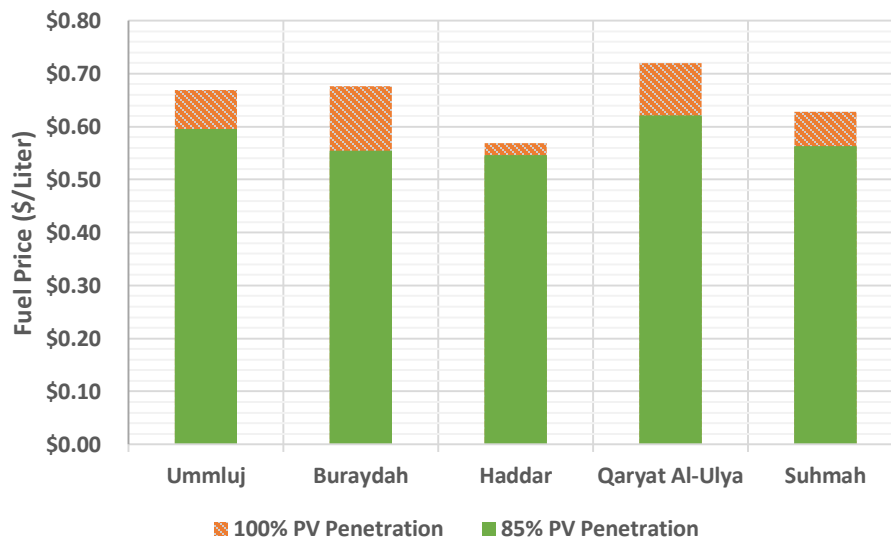


Figure 32. Breakeven Points for Different Locations for Batch Mode

5.4.5. Effect of Second Storage Tank Salinity:

In the previous work, all analyses was conducted to serve 1000 people for two purposes: drinking and household applications. The salinity aimed for household water is 1000 *ppm*. However, results will change with changing this salinity. This section demonstrates the effect of second storage tank salinity on the systems. Table 22 represents the effect of second storage tank salinity on the RO design. As the salinity increases the permeate flow rate, number of membrane elements, number of pressure vessels and costs decreases. Figure 33 illustrates the effect of second storage tank salinity on the LCOW for different locations at 100% PV penetration and batch mode. Results show that 10% reduction on LCOW are achieved if the second tank salinity is increased by 500 *ppm* and vice versa. The reason behind this is that as the second storage salinity increased, more feed water can be mixed directly without desalination. This will reduce the RO capacity and energy consumption. In other aspect, the SEC decreases as the second storage tank salinity increases. Figure 34 shows that if the salinity rise 500 *ppm*, SEC of the system will decrease 5%.

Table 22. Effect of Second Storage Tank Salinity on the RO Design

Mode	Second Tank Salinity (ppm)	Permeate Flow Rate ($\frac{m^3}{h}$)	No. of Membranes	No. of PV	Annual Capital Cost (\$)	Annual operation Cost (\$)
Batch	500	37.96	35	6	14,003.41	11,612.31
	1000	34.3	31	5	12,687.86	11,526.02
	1500	30.91	28	5	11,469.35	11,446.09
Continuous	500	7.85	8	1	3,047.95	10,322.75
	1000	7.14	7	1	2,792.75	10,306.01
	1500	6.44	6	1	2,541.14	10,289.50

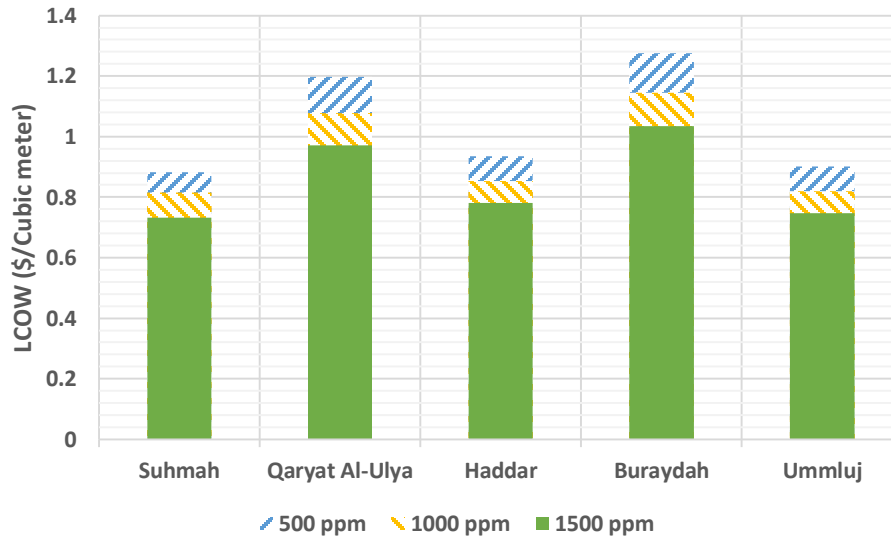


Figure 33. Effect of Second Storage Tank Salinity on the LCOW for Different Locations at 100% PV Batch Mode

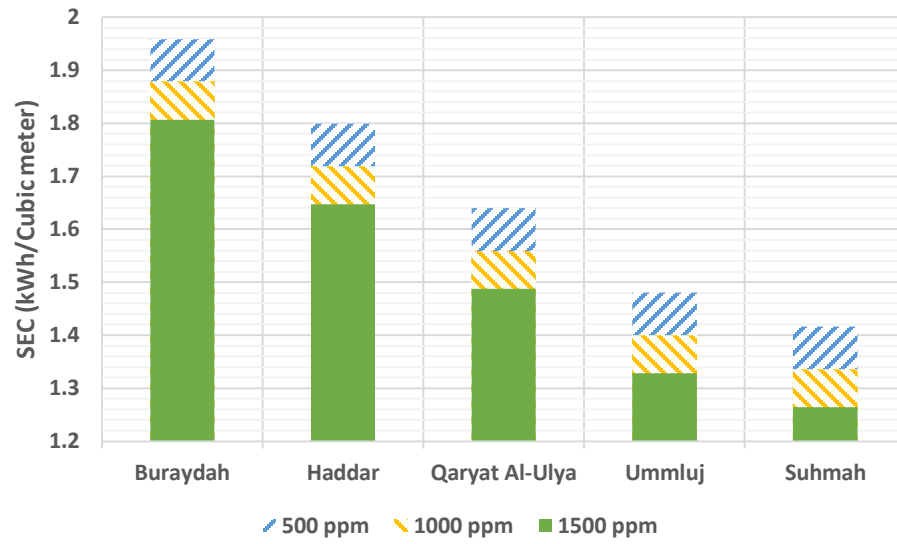


Figure 34. Effect of Second Storage Tank Salinity on the SEC for Different Locations at 100% PV Batch Mode

Chapter 6:

Conclusion and Recommendations

6.1. Conclusion:

In conclusion, the aim of this study is to analyze RO systems powered by hybrid diesel-PV to desalinate wells water in five locations in Saudi. Performance and cost analyses are conducted to find the optimum RO and power system. In RO analyses, two modes are compared: batch mode that operates 5 hours a day and continuous mode that operates 24 hours a day. In each mode, the benefits of adding second storage tank ,PX and second stage for RO system are studied. For the power analyses, the effect of increasing PV penetration in the system is performed, starting from 0% up to 100%. In addition, the effect of fuel price is analyzed. Results can be summarized in the following points:

- Adding second storage tank for household purposes, with 1000 *ppm* salinity, results in 11% discount in the LCOW.
- Using PX as ERD in one stage RO system leads to 26% reduction in the SEC. However, it is feasible to add it in continuous mode, but not feasible in batch mode.

- Adding second stage reduced the SEC by 22% and increased the water recovery by 15%.
- In general, the two stages case is the optimum case from performance and cost point of view.
- The optimum mode is the continuous mode if the PV penetration is 40% and less for all locations.
- The optimum mode is the batch mode if the PV penetration is more than 40% for all locations.
- In batch mode, 85% PV penetration has the lowest LCOW with good PV sharing.
- Haddar has the best environmental resources and climate conditions for PV applications.
- At today fuel price in KSA, it is not economically feasible to add PV to the system.
- In general, the breakeven point for the fuel price, that makes adding PV to the system feasible, is \$0.58 per liter. Haddar has the lowest breakeven point, which is \$0.55 per liter. For comparison purpose, the fuel prices in UEA and Oman are \$0.78 per liter and \$0.67 per liter, respectively.
- Second storage tank salinity has a real impact on the SEC and LCOW. For instant, 5% reduction in the SEC and 10% reduction in the LCOW when the salinity increased by 500 *ppm*.

6.2. Recommendations:

This study has three main limitations: the well salinity, the production size and the number of operation hours in batch mode. Therefore, this study could be expanded to cover the following:

- Study Different well salinity.
- Analyze Larger RO systems.
- Find the optimum operation hours for the batch mode.

In order to make the PV power system more feasible, the following points should be considered:

- Finding a way to use the PV exceed electricity.
- Increasing the efficiency of PV panels.

In the near future, three main parameters may change which will make PV power system more feasible:

- Decreasing in PV cost.
- Increasing in fuel cost.
- Enacting of emissions penalty law.

References

- [1] J. Kucera, *Desalination: Water from Water*, Beverly: Scrivener, 2014.
- [2] M. Tran, E. Koncagul and R. Connor, "The United Nations World Water Development Report 2016," 2016.
- [3] "Statistical Report of Ministry of Water and Electricity Report," 2017.
- [4] H. T. El-Dessouky and H. M. Ettouney, *Fundamentals of Salt Water Desalination*, The Netherlands: ELSEVIER, 2002.
- [5] Dow, FILMTEC™ Reverse Osmosis Membranes, Technical Manual, Dow Water & Process Solutions.
- [6] "Energy Recovery Company," [Online]. Available: <http://www.energyrecovery.com/>.
- [7] S. Alawaji, M. S. Smiai and S. Rafique, "PV-Powered Water Pumping and Desalination Plant for Remote Areas in Saudi Arabia," *Applied Energ*, vol. 52, pp. 283-289, 1995.
- [8] S. A. ALAJLAN and M. S. SMIAI, "Performance and Development of PV - Plant for Water Pumping and Desalination for Remote Area in Saudi Arabia," 1996.
- [9] D. B. Riffela and P. C. Carvalho, "Small-scale photovoltaic-powered reverse osmosis plant without batteries: Design and simulation," *Desalination*, vol. 247, pp. 378-389, 2009.
- [10] H. Elasaad, A. Bilton, L. Kelley, O. Duayhe and S. Dubowsky, "Field evaluation of a community scale solar powered water purification technology: A case study of a remote Mexican community application," *Desalination*, vol. 375, pp. 71-80, 2015.
- [11] L. Karimi, L. Abkar, M. Aghajani and A. Ghassemi, "Technical feasibility comparison of off-grid PV-EDR and PV-RO desalination systems via their energy consumption," *Separation and Purification Technology*, vol. 151, pp. 82-94, 2015.
- [12] B. Peñate, Vicente J. Subiela, F. Vega, F. Castellano, F. J. Domínguez and V. Millán, "Uninterrupted eight-year operation of the autonomous solar photovoltaic reverse osmosis system in Ksar Ghilène (Tunisia)," *Desalination and Water Treatment*, vol. 55, p. 3141–3148, 2015.
- [13] S. Abdallah, M. Abu-Hilal and M. S. Mohsen, "Performance of a photovoltaic powered reverse osmosis system under local climatic conditions," *Desalination*, vol. 183, pp. 95-104, 2005.

- [14] P. Poovanaesvaran, M. Alghoul, K. Sopian, N. Amin, M. Fadhel and M. Yahya, "Design aspects of small-scale photovoltaic brackish water reverse osmosis (PV-BWRO) system," *Desalination and Water Treatment*, vol. 27, p. 210–223, 2011.
- [15] A. M. Bilton, R. Wiesman, A. Arif, S. M. Zubair and S. Dubowsky, "On the feasibility of community-scale photovoltaic-powered reverse osmosis desalination systems for remote locations," *Renewable Energy*, vol. 36, pp. 3246–3256, 2011.
- [16] D. P. Clarke, Y. M. Al-Abdeli and G. Kothapalli, "The effects of including intricacies in the modelling of a small-scale solar-PV reverse osmosis desalination system," *Desalination*, vol. 311, pp. 127–136, 2013.
- [17] P. Poovanaesvaran, M. Alghoul, A. Fadhil, M. Abdul-Majeed, N. Assim and K. Sopian, "Techno-economic evaluation of a small-scale PVBWRO system at different latitudes," *Desalination and Water Treatment*, vol. 52, p. 7082–7091, 2014.
- [18] S. Kumarasamy, S. Narasimhan and S. Narasimhan, "Optimal operation of battery-less solar powered reverse osmosis plant for desalination," *Desalination*, vol. 375, pp. 89–99, 2015.
- [19] B. S. Richards, D. P. Capão, W. G. Früh and A. I. Schäfer, "Renewable energy powered membrane technology: Impact of solar irradiance fluctuations on performance of a brackish water reverse osmosis system," *Separation and Purification Technology*, vol. 156, pp. 379–390, 2015.
- [20] N. Ahmad, A. K. Sheikh, P. G. a and M. Elshafie, "Modeling, simulation and performance evaluation of a community scale PVRO water desalination system operated by fixed and tracking PV panels: A case study for Dhahran city, Saudi Arabia," *Renewable Energy*, vol. 75, pp. 433–447, 2015.
- [21] H. D. Raval and S. Maiti, "Ultra-low energy reverse osmosis with thermal energy recovery from photovoltaic panel cooling and TFC RO membrane modification," *Desalination and Water Treatment*, vol. 57, p. 4303–4312, 2016.
- [22] M. Thomson and D. Infield, "A photovoltaic-powered seawater reverse-osmosis system without batteries," *Desalination*, vol. 153, pp. 1–8, 2002.
- [23] G. Ahmad and J. Schmid, "Feasibility study of brackish water desalination in the Egyptian deserts and rural regions using PV systems," *Energy Conversion and Management*, vol. 43, p. 2641–2649, 2002.

- [24] A. Helal, S. Al-Malek and E. Al-Katheeri, "Economic feasibility of alternative designs of a PV-RO desalination unit for remote areas in the United Arab Emirates," *Desalination*, vol. 221, pp. 1-16, 2008.
- [25] I. Zeiner, J. A. Suul, A. Marcos and M. Molinas, "System Design and Load Profile Shaping for a Reverse Osmosis Desalination Plant Powered by a Stand-Alone PV System in Pozo Colorado, Paraguay," in *Ninth International Conference on Ecological Vehicles and Renewable Energies (EVER)*, 2014.
- [26] I. Zeiner, J. A. Suul and M. Molinas, "Competitiveness of Grid Connected Photovoltaic Power Supply for a Desalination Plant under a Prospective Power Market in Paraguay," in *The 2nd IEEE Conference on Power Engineering and Renewable Energy*, 2014.
- [27] A. M. Bilton and L. C. Kelley, "Design of power systems for reverse osmosis desalination in remote communities," *Desalination and Water Treatment*, vol. 55, p. 2868–2883, 2015.
- [28] M. C. Garg and H. Joshi, "Optimization and economic analysis of small scale nanofiltration and reverse osmosis brackish water system powered by photovoltaics," *Desalination*, vol. 353, pp. 57-74, 2014.
- [29] D. E. A. Zaid, "Economic analysis of a stand-alone reverse osmosis desalination unit powered by photovoltaic for possible application in the northwest coast of Egypt," *Desalination and Water Treatment*, vol. 54, p. 3211–3217, 2015.
- [30] M. Alghoul, P. Poovanaesvaran, M. Mohammed, A. Fadhil and A. Muftah, "Design and experimental performance of brackish water reverse osmosis desalination unit powered by 2 kW photovoltaic system," *Renewable Energy*, vol. 93, pp. 101-114, 2016.
- [31] J. Shen, B. S. Richards and A. I. Schäfer, "Renewable energy powered membrane technology: Case study of St. Dorcas borehole in Tanzania demonstrating fluoride removal via nanofiltration/reverse osmosis," *Separation and Purification Technology*, vol. 170, pp. 445-452, 2016.
- [32] V. Fthenakis, A. A. Atia, O. Morin, R. Bkayrat and P. Sinha, "New prospects for PV powered water desalination plants: case studies in Saudi Arabia," *PROGRESS IN PHOTOVOLTAICS: RESEARCH AND APPLICATIONS*, vol. 24, p. 543–550, 2016.
- [33] M. Jones, I. Odeh, M. Haddad, A. Mohammad and J. Quinn, "Economic analysis of photovoltaic (PV) powered water pumping and desalination without energy storage for agriculture," *Desalination*, vol. 387, pp. 35-45, 2016.

- [34] I. J. Esfahani and C. Yoo, "An optimization algorithm-based pinch analysis and GA for an off-grid batteryless photovoltaic-powered reverse osmosis desalination system," *Renewable Energy*, vol. 91, pp. 233-248, 2016.
- [35] "HOMER Help Manual," HOMER Energy, 2016.
- [36] "NASA Surface Meteorology and Solar Energy data," NASA, [Online]. Available: <https://power.larc.nasa.gov/>.
- [37] "DESALINATION, Products Catalog," Energy Recovery Company, 2018.

Vitae

Name :[Abdalmajeed Khalid Al-Rubayan]

Nationality :[Saudi]

Date of Birth :[5/18/1991]

Email :[aalrubayan@KACST.edu.sa]

Address :[Saudi Arabia - Riyadh]

Academic Background :[

M.Sc. Mechanical Engineering: King Fahd University of Petroleum and Minerals
(KFUPM), Dhahran, Saudi Arabia 2018]

B.S Mechanical Engineering: King Fahd University of Petroleum and Minerals
(KFUPM), Dhahran, Saudi Arabia 2014

Research interest:

Thermal sciences, Heat transfer, Solar Energy, and Reliability.

Experience:

PV reliability lab engineer (2014-2016)

Researcher at Water and Energy Institute in KACST (2014-2018)